UCID-18334

BUILDUP STUDIES FOR MFTF-B

James M. Gilmore

April 23, 1980

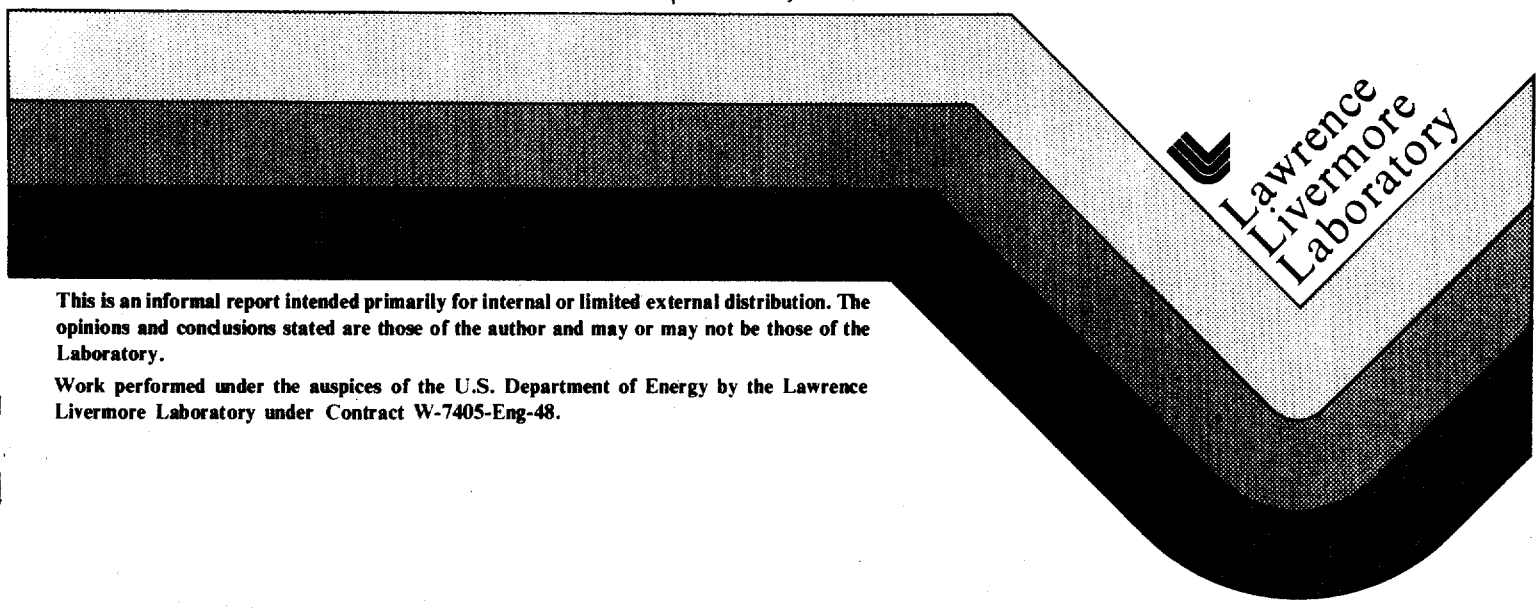

Work performed under the auspices of the U.S. Department of Energy by the Lawrence Livermore Laboratory under Contract W-7405-Eng-48.

BUILDUP STUDIES FOR MFTF-B

James M. Gilmore

A one-dimensional radial transport code[1] which was developed to study radial transport in tandem mirror machines has been used to perform buildup studies for the central-cell plasma of the proposed MFTF-B experiment at Lawrence Livermore Laboratory. The effects of the cold, unpumped, neutral gas (which accompanies the hot, neutral-beam injection in the central cell) upon the central-cell plasma have been studied for the low $\varepsilon(\varepsilon \equiv (\Omega_{pi}/\Omega_{ci})2)$ mode[2,3] and for the two-component mode. A mode here is defined as a particular set of parameters (density, temperature, etc.) under which the experiment will be performed. A very preliminary study of the effects of plateau resonant transport[4] upon the equilibrium plasma obtained for the low-ε mode of operation has also been performed.

The results obtained indicate that central-cell plasma buildup to the desired operating conditions of both the low-ε and two-component modes can be achieved provided that the spatial and temporal behavior of the neutral-gas profiles is properly adjusted. Furthermore, the results indicate that, within the framework of the physics included in the code, buildup will occur if the cold, unpumped-gas density at the central-cell-plasma edge does not exceed approximately 1.6×10^9 cm^{-3} for the low-ε mode, or 1.6×10^{10} cm^{-3} for the two-component mode. Also, in the case of the low-ε mode, it is desirable that the source gas stream upon which the initial cold, low density plasma is allowed to build up must be initially of high density (1.6×10^{10} cm^{-3}) so that the plasma density will build up rapidly (on the order of 10^{-2} seconds). Once the desired center-line density ($\tilde{=}1.7 \times 10^{12}$ cm^{-3}) has been achieved, the source gas density must be cut back ($\tilde{=}1.6 \times 10^6$ cm^{-3}) in order to allow the central-cell ions to heat to the desired final temperature ($\tilde{=}2.2$ keV).

The two-component-mode studies are based upon a source gas stream which is adjusted to yield an ion source constant in radius and time and sufficient to sustain the plasma equilibrium against end-loss.

Section I of this report describes MFTF-B operation parameters and the physics upon which the code is based, and discusses its limitations. The

thermal barrier physics[5] is not included in the present physical model. Section II describes the buildup scenarios which have proven successful computationally and gives reasons for their success. Section III presents the results which have been obtained and discusses their significance. Section V presents in detail the transport equations which are numerically solved. Section VI gives some details of the equations used to solve for the radial dependence of the neutral-gas density. Section VII briefly discusses the method used to solve for the potential, designated ϕ_e, which is the potential difference between the middle of the central cell and infinity. Section IV is the conclusion.

SECTION I. MFTF-B PARAMETERS AND OVERVIEW OF THE PHYSICAL MODEL

Tables I and II give the machine and plasma parameters upon which the buildup study is based. A more detailed discussion of MFTF-B parameters may be found in Refs. 2 and 3. Table II gives the center line values for the initial plasma parameters from which the buildup is taken to proceed for both the low-ε and the two-component modes. The initial temperature profiles for both the central-cell ions and electrons are taken to be both constant, as a function of plasma radius, and flat. The boundary conditions used are fixed gradient with $1/u\ du/dr = \alpha$. Typically $\alpha = 0$ or 0.6 (here u is a density or a temperature). The initial profiles are presented graphically in Fig. 1 of Section III. The initial plug temperature (and hence energy profile) is constant in time and flat as a function of central cell plasma radius, with $T_p = 2/3\ E_p = 2/3\ E_{inj}$, where the subscript p refers to plug and E_{inj} is the injection energy of the plug ions, taken to be the neutral beam injection energy.

The initial central cell ion density profile is taken to be

$$n_i(r) = n_i[1 - (r/r_c)^2] \tag{1.1}$$

(n_i is given in Table III). The same spatial behavior is imposed upon the plug-ion density for all times $t \geq 0$, the plug density being normalized to vanish on the field line corresponding to the edge of the central cell plasma (i.e., replace n_i by n_p in (1.1), taking n_p from Table III).

The physical model used to describe the plasma in the central cell of the MFTF-B machine is essentially the same as that described in detail in Ref. 1. The only significant difference lies in the equation in use in the present model for bounce-averaged electron temperature. This equation has been modified to agree with the zero dimensional equation given in Ref. 6, in which the energy change associated with a time dependent potential has been included. The relevant equation in Ref. 6 is equation (A9) in which the term $(dN_{ec}/dt)_{e\ell}$ is taken to be the difference, at any given radial position, between electron sources and sinks and ion sources and sinks, plus end-loss of central-cell ions, all per unit flux tube. The equations which are used to describe the time evolution of the plasma densities and temperatures are given in some detail in Section V. The classical transport coefficients used are those of Braginskii[7] and the neo-classical, plateau-resonant-transport coefficients used are rough approximations to the diagonal coefficients given in Ref. 4. The exact form of the plateau-resonant-transport coefficients is given in Section V.

The plug plasma is assumed to have reached an equilibrium with the densities and temperatures given in Tables I - III. The plug ion loss is therefore the plug source, and is given by:

$$S_p = nA\,\tau_{DR}\,\ell n\left(\frac{E_{inj} - 3/2\,T_e}{E_{out} - 3/2\,T_e}\right), \tag{1.2}$$

where

$$E_{out} = MAX\left(C\,T_e^{3/2}/E_p^{1/2},\ \frac{\phi_i + \phi_e}{R_p - 1}\right), \tag{1.3}$$

$C = 48$ for deuterium plugs

$n = 1$

$A = 1$

$\tau_{DR} \equiv$ classical Spitzer drag time.

The potential, ϕ_i, between the center of the central cell and the plug is determined by assuming Maxwell-Boltzmann electrons free-streaming along field lines:

Table I. Low ε Mode Parameters (Center-Line Values) (Equilibrium)

Electrons	
Temperature, T_e - keV	5.5
Potential, ϕ_e - keV	28
Plug Ions	
Density, n_p - cm^{-3}	1.4×10^{13}
Mean energy, E_p - keV	100
Radius, r_p - cm	40
Length, L_p - cm	100
Vacuum magnetic field, B_p - kG	20
Vacuum mirror ratio, R_p	2
Central Cell Ions	
Density, n_c - cm^{-3}	$\sim 1.7 \times 10^{12}$ - 2×10^{12}
Temperature, T_i - keV	~2.2
Potential, ϕ_i - keV	10.8
Radius, r_c - cm	80
Length, L_c - cm	2500
Vacuum magnetic field, B_s - kG	5
Cold unpumped neutral gas density	
$t < 0.5$ sec, n_1 - cm^{-3}	1.6×10^9 (maximum)
$t \geq 0.5$ sec, n_1 - cm^{-3}	0
Cold stream neutral density, n_2 - cm^{-3}	1.6×10^{10}
($n_i \leq 1.6 \times 10^{12}$ cm^{-3})	
($n_i > 1.6 \times 10^{12}$ cm^{-3}), n_2 - cm^{-3}	1.6×10^6

Note: The unpumped neutral gas density is taken to be zero for times greater than 0.5 sec as 0.5 sec is the projected time duration of central cell neutral beam injection.

Table II. Two Component Mode Parameters (Center Line Values) (Equilibrium)

Electrons	
Temperatures, T_e - keV	0.81
Potential, ϕ_e - keV	5
Plug Ions	
Density, n_p - cm^{-3}	9.8×10^{13}
Mean energy, E_p - keV	50
Radius, r_p - cm	40
Length, L_p - cm	100
Vacuum magnetic field, B_p - kG	20
Vacuum mirror ratio, R_p	2
Central Cell Ions	
Density, n_c - cm^{-3}	4.1×10^{13} cm^{-3}
Temperature, T_i - keV	0.16
Potential, ϕ_i - keV	0.79
Radius, r_c - cm	34
Length, L_c - cm	2500
Vacuum magnetic field, B_s - kG	5
Trapped ion source - cm^{-3} s^{-1}	1.03×10^{15}
Unpumped gas density $t < 0.5$ sec, n_2 - cm^{-3}	1.6×10^{10}
$t \geq 0.5$ sec n_2 - cm^{-3}	0

Table III. Initial Plasma Parameters (Center Line Values)

Electrons	
Temperature, T_e - keV	0.01
Potential, ϕ_e - keV	0.047
Plug Ions	
Density, n_{ps} - cm^{-3}	1×10^{12}
n_{po} - cm^{-3}	1.4×10^{13}
where: $n_p(r,t) = n_{po}(1 - e^{-\alpha t})[1 - (r/r_c)^2] + n_{ps}[1 - (r/r_c)^2]$	
α, s^{-1}	$1 \times 10^2 - 1 \times 10^3$
Mean energy, E_p - keV	100 (low ε)
	50 (two component)
Central Cell Ions	
Density, n_i - cm^{-3}	2.5×10^{11}
Temperature, T_i - keV	0.05
Potential, ϕ_i - keV	0.018

$$\phi_i = T_e \ell n \left(\sum_{\substack{\text{plug} \\ \text{ion} \\ \text{species}}} z_i n_i \Big/ \sum_{\substack{\text{central} \\ \text{cell ion} \\ \text{species}}} z_i n_i \right) z_i n_i \quad . \tag{1.4}$$

The potential, ϕ_e, between the central cell and infinity, is determined by equating total electron loss per unit flux tube (both radial and axial) to total ion loss per unit flux tube (both radial and axial):

$$\frac{dN}{dt} = L_s \frac{dn_i}{dt} \quad , \tag{1.5}$$

N ≡ total number of electrons per unit flux tube.

In the case of the low-ε mode, the plugs are assumed to be gradient stabilized against the DCLC mode. The two-component mode depends upon warm plasma streaming from the central cell into the plugs to provide the requisite stabilization. However, in the case of results presented it is simply assumed that there exists sufficient central-cell end loss to provide for DCLC stable plugs. No checks are made here beyond those done in Ref. 2.

The neutral-gas physics used to model the burn-up of the neutral gas during plasma buildup is fairly simple. First, the gas incident on the central-cell plasma from both the source gas feed streaming in from the fans, against which the plasma builds up, and the cold gas which accompanies the hot, neutral-beam injection is D_2^o (neutral, diatomic deuterium gas). It is assumed that the mean, free path of the D_2^o is much less than the radius of the central cell plasma and hence all of the D_2^o is assumed to interact essentially at the plasma edge to yield D_{FC}^o (monoatomic, neutral-deuterium gas resulting from a Franck-Condon process) of energy 3 eV. Therefore, all neutral-gas densities referred to previously and subsequently are to be taken to be D_{FC}^o densities. It is assumed that the dominant reaction mechanism for production of D_{FC}^o from cold D_2^o at the plasma edge is $D_2^o \rightarrow D_{FC}^o + \not{D}^+$, by either electron impact or ion impact. It is then assumed that a total energy loss of about 37 eV per ionization of the resulting D_{FC}^o is paid by either the ions or electrons. The arrow indicates that no account is taken of the D^+. The description above is clearly a gross approximation, since there are several possible reactions

which the D_2^o can undergo. This approach was adopted in an attempt to simulate, to some extent, the energy drain on the ions and electrons due to plasma-D_2^o and plasma-D_{FC}^o interactions.

The D_{FC}^o flux which results from the D_2^o interacting at the plasma edge is assumed to be born with a monodirectional, inwardly-directed velocity towards the plasma center. This flux is actually born isotropically. Hence, the model used underestimates the virgin (non-interacted) neutral flux at the plasma edge. Furthermore, it is assumed that all first-generation, charge-exchange neutrals which result from charge-exchange reactions between the virgin neutrals and the plasma ions are immediately lost from the plasma. This approximation might be good for a hot, low-density plasma, but since the plasmas being simulated are not hot, sparce plasmas (especially at the inception of plasma buildup), the model used clearly underestimates the neutral flux in the plasma interior.

There are provisions in the neutral physics for the inclusion of so-called finite-Larmor-radius (FLR) corrections to the ion source and loss terms which result from charge exchange and ionization.[8] These corrections involve the averaging of ion source and loss terms over the ion-Larmor orbit, the size of the orbit being determined by the neutral gas energy. For Franck-Condon deuterium neutrals of energy 3 eV in a 5-kG field, one finds a Larmor radius of approximately 0.07 cm, which is clearly negligible in comparison with the plasma radius. Hence, the finite-Larmor-radius corrections should not be significant for the virgin neutrals. This conclusion is borne out by the code results given in Section III. These corrections would be significant, however, for the hot neutrals which would result from following several generations of charge exchange. There is, how- ever, no way of including this effect in the present neutral model.

Finally, the model assumes that all the relevant neutral time scales are fast when compared with all of the plasma time scales. Hence, at all times it may be assumed that the neutrals have reached a steady state and that the density of neutral species ℓ at any point in the plasma can be found by using:

$$v_\ell \frac{\partial n_\ell}{\partial x} = -\beta_\ell n_\ell + G(n_\ell) , \qquad (1.6)$$

$v \equiv$ velocity of neutral species

$\beta_\ell \equiv$ coefficient of those source or sink terms proportional to n_e

$G(n_\ell) \equiv$ all other sources or sinks.

The details of β_ℓ and $G(n_\ell)$ are given in Section VI.

SECTION II. THE BUILDUP SCENARIO

The successful buildup scenario for the low-ε mode simulations has been found to be the following: the neutral gas density of the source gas streaming into the central cell from the end fans is taken to be constant in space and time and of magnitude 1.6×10^{10} cm^{-3} until central cell buildup to approximately 1.7×10^{12} cm^{-3} has been achieved at the center of the plasma. Once center-line buildup has been achieved, the source gas density is reduced to 1.6×10^{6} cm^{-3}, constant in space and time. This lower final density is chosen so that the ion source, which is given by

$$S_i = n_i n_g \langle \sigma v \rangle \tag{2.1}$$

is sufficient to sustain the plasma against end-loss. Note that $\langle \sigma v \rangle \equiv \sum \langle \sigma v \rangle_i$ is the reaction rate for impact ionization by ions and electrons. The end-loss is given by formulas similar to Pastukhov's,[1,6] and the $\langle \sigma v \rangle$ values are calculated using the subroutine described in Ref. 9.

The reason that is it necessary to have an initially high, neutral-gas background which is then reduced to a lower level becomes apparent when simplified equations for the ion temperature equilibration in the central cell are analyzed. The ion temperature equilibration can be approximately described by:

$$\frac{\partial T_i}{\partial t} \cong - T_i n_\ell \langle \sigma v \rangle + \bar{\nu}_\varepsilon^{\,i/e} (T_e - T_i) \ , \tag{2.2}$$

$$\bar{\nu}_\varepsilon^{\,\alpha/\beta} = \frac{1.8 \times 10^{-19} \, (m_\alpha \, m_\beta)^{1/2} \, z_\alpha^{\,2} \, z_\beta^{\,2} \, \lambda_{\alpha\beta} n_\beta}{(m_\alpha \, T_\beta + m_\beta \, T_\alpha)^{3/2}} \ \text{s}^{-1} \ . \tag{2.3}$$

$\lambda_{\alpha\beta}$ = Coulomb Log

T_α, T_β in eV

Equation (2.2) is an approximation in that radial and axial losses have been completely neglected, as has been all radial dependence of the temperature and density profiles. For low temperatures and high ambipolar potentials, which correspond to the initial phases of buildup, the neglect of end-loss is particularly good (see Section V), and it has been found that radial-temperature conduction and convection are not large, particularly for flat profiles. Therefore Eq. (2.2) can shed some light on the temperature equilibration process, although it is admittedly a gross approximation.

If the temperature and density dependence of $\langle\sigma v\rangle$ and $\nu_\varepsilon^{i/e}$ is now ignored, and a constant, neutral-gas density n_ℓ is assumed, as well as a time-independent, electron temperature, T_e, Eq. (2.2) may be solved:

$$T_i(t) \cong T_i(t=0)e^{-(\bar{\nu}_\varepsilon^{i/e} + n_\ell \langle\sigma v\rangle)t} + \frac{T_e \bar{\nu}_\varepsilon^{i/e}}{\bar{\nu}_\varepsilon^{i/e} + n_\ell \langle\sigma v\rangle)} \left(1 - e^{-(\nu_\varepsilon^{i/e} + n_\ell \langle\sigma v\rangle)t}\right) . \qquad (2.4)$$

It can immediately be seen that if $n_\ell \langle\sigma v\rangle \gg \bar{\nu}_\varepsilon^{i/e}$, there is no hope of achieving equilibrium ion temperatures on the order of the electron temperatures. Using Eq. (2.3) with T_e = 100 eV, $\lambda_{ei} \cong 14$, $m_i = 3.34 \times 10^{-24}$ g, $n_e \cong n_i \cong 1 \times 10^{12}$ cm^{-3}, $m_e = 9.11 \times 10^{-28}$ g, a classical inverse drag time of $\bar{\nu}_\varepsilon^{i/e} \cong 22\text{s}^{-1}$ is obtained. For $\langle\sigma v\rangle \cong 10^{-7}$ cm^3 s^{-1} and $n_\ell = 1 \times 10^{10}$ cm^{-3}, $n_\ell \langle\sigma v\rangle = 1 \times 10^3$ s$^{-1} \gg \bar{\nu}_\varepsilon^{i/e}$. For $n_\ell = 1 \times 10^6$ cm^{-3}, $n_\ell \langle\sigma v\rangle = 0.1 \ll \bar{\nu}_\varepsilon^{i/e}$. Therefore, the higher neutral-gas density, which enables a rapid buildup of the central-cell plasma but which also cools off the ions, must be reduced to a value which yields an $n_\ell \langle\sigma v\rangle$ value on the order $\bar{\nu}_\varepsilon^{i/e}$ in order for significant central-cell ion heating to occur. The same equilibrium could be achieved by using lower initial gas densities and allowing the buildup to occur over much longer time scales. This method is not computationally feasible and it is in all likelihood experimentally undesirable also.

For the case in which the source-neutral-gas density is adjusted to yield a constant ion source of magnitude α cm^{-3} s^{-1}:

$$\frac{\partial T_i}{\partial t} \cong (T_i - T_e)\, \bar{\nu}_{\varepsilon}^{\,i/e} - \frac{\alpha}{n_i} T_i \quad ; \tag{2.5}$$

$$n_i(t) = n_i(t = 0) + \alpha t \quad ; \tag{2.6}$$

$$T_i(t) = \frac{n_i(t = 0)}{n_i(t = 0) + \alpha t} \; T_e \left(1 - e^{-\bar{\nu}_{\varepsilon}^{\,e/i} t}\right)$$

$$+ \frac{\alpha T_e}{n_i(t = 0) + \alpha t} \left\{ t - (\bar{\nu}_{\varepsilon}^{\,e/i})^{-1} \left(1 - e^{-\bar{\nu}_{\varepsilon}^{\,e/i} t}\right) \right\} + T_i(t = 0). \tag{2.7}$$

Therefore, in the case of the two-component-mode simulation, in which a constant ion source is imposed, the central-cell ion temperature, T_i, will equilibrate at T_e, but the equilibration will be linear in time rather than exponential, and will occur on a time scale such at $\alpha t >> n_i(t = 0)$.

The preceding, admittedly simple analysis demonstrates the desirability of choosing the buildup scenario which has been used. Whether or not such a scenario is physically realizable is certainly an open question.

The neutral-gas density meant to simulate that of the unpumped cold D_2^o (equivalent D_{FC}^o) which will accompany the hot neutral-beam injection in the central cell is taken to be 1.6×10^9 cm^{-3} at the plasma edge for the low-ε mode and 1.6×10^{10} cm^{-3} at the plasma edge for the two-component mode. These values are the maximum that the physics now in the code indicates that the plasma will tolerate. Higher, unpumped neutral-gas densities permit the central-cell plasma edge to build up above the plug edge density. This buildup is therefore sufficiently rapid to overcome the tendency of the plasma to stream out the ends of the center cell. Once the central-cell density on any given field line has built up above the plug density, the code physics breaks down irrevocably. The edge density is integrated

across the width of the plasma using Eq. (1.6). The unpumped neutral gas is assumed incident upon the central-cell plasma for the projected duration of the neutral-beam injection--0.5 seconds. It should be noted that a density of 1.6×10^9 cm^{-3} at 3 eV corresponds to 274 A of equivalent current for the low-ε mode and a density of 1.6×10^{10} cm^{-3} corresponds to an equivalent current of 1370 A for the two-component mode.

SECTION III. RESULTS OF THE BUILDUP CALCULATION

The primary problem investigated has been the effect of the unpumped neutral gas which accompanies the hot, neutral-beam injection in the central cell upon the central-cell plasma. Computer simulations of the time behavior of the central-cell plasma have been performed for unpumped gas densities at the plasma edge ranging from 0 cm^{-3} to 1.6×10^9 cm^{-3} for the low-ε mode, and 1.6×10^{10} cm^{-3} for the two-component mode. Table IV summarizes the parameters of the cases which have been studied. Figures 1-25 present the results which have been obtained.

It is seen that a high density, cool, loss-prone (in that ϕ_i and ϕ_e are low) plasma develops at the plasma edge for those cases (MF01 and MF06) in which the density of the unpumped neutral gas is relatively high. The ragged portions of the profiles are numerical and not physical. In these density regimes the code was operating near the permissible limits set by the Courant condition.[10] It should also be noted that a comparison of MF01 and MF06 bears out the earlier conclusion that the FLR corrections are not important for the neutral-gas model being employed, since the results of these cases do not significantly differ.

Those cases in which the density of the unpumped neutral gas is lower than 1.6×10^9 cm^{-3} (MF02, MF03, and MF05) show that in this density regime the effect of the unpumped neutral gas is unimportant. Furthermore, all the cases exhibit the fact that the equilibrium plasma in effect forgets that the unpumped neutral gas (high or low density) was ever present; the system recovers from the negative effects of the gas. A case in which the effects of a slower plug rise time and slightly less-dense plug plasma were studied is shown in MF04. No significant difference from the other cases is exhibited.

Table IV. Summary of Case Parameters

Label of Case	Parameters
MF01	$n_s = 1.6 \times 10^{10}$ cm^{-3}, 1.6×10^{6} cm^{-3} $n_u = 1.6 \times 1^{-9}$ cm^{-3} FLR $\alpha_p = 1 \times 10^{3}$ s^{-1} $n_p(r = 0) = 1.4 \times 10^{13}$ cm^{-3}
MF02	$n_s = 1.6 \times 10^{10}$ cm^{-3}, 1.6×10^{6} cm^{-3} $n_u = 1.6 \times 10^{8}$ cm^{-3} FLR $\alpha_p = 1 \times 10^{13}$ cm^{-3} $n_p(r = 0) = 1.4 \times 10^{13}$ cm^{-3}
MF03	$n_s = 1.6 \times 10^{10}$ cm^{-3}, 1.6×10^{6} cm^{-3} $n_u = 1.6 \times 10^{6}$ cm^{-3} FLR $\alpha_p = 1 \times 10^{3}$ s^{-1} $n_p(r = 0) = 1.4 \times 10^{13}$ cm^{-3}
MF04	$n_s = 1.6 \times 10^{10}$ cm^{-3}, 1.6×10^{6} cm^{-3} $n_u = 1.6 \times 10^{9}$ cm^{-3} NO FLR $\alpha_p = 1 \times 10^{2}$ s^{-1} $n_p(r = 0) = 1.0 \times 10^{13}$ cm^{-3}
MF05	$n_s = 1.6 \times 10^{10}$ cm^{-3}, 1.6×10^{6} cm^{-3} $n_u = 1.6 \times 10^{9}$ cm^{-3} $\alpha_p = 1 \times 10^{3}$ s^{-1} $n_p(r = 0) = 1.4 \times 10^{13}$ cm^{-3} FLR
MF06	$n_s = 1.6 \times 10^{10}$ cm^{-3}, 1.6×10^{6} cm^{-3} $n_u = 1.6 \times 10^{9}$ cm^{-3} NO FLR $\alpha_p = 1 \times 10^{3}$ s^{-1} $n_p(r = 0) = 1.4 \times 10^{13}$ cm^{-3}
MF08A	MF06 equilibrium with neo-classical plateau resonant transport
MF09	MF06 equilibrium with solely classical transport
MF11 (two component simulation)	α_s(source) $= 1.05 \times 10^{15}$ cm^{-3} s^{-1} $n_u = 1.6 \times 10^{10}$ cm^{-3} NO FLR $n_p(r = 0) = 9.8 \times 10^{13}$ cm^{-3} $\alpha_p = 1 \times 10^{3}$

Note: $n_s \equiv$ stream neutral gas density
$n_u \equiv$ unpumped neutral gas density
$\alpha_p \equiv$ plug inverse rise time
$n_p(r = 0) \equiv$ center line plug ion density

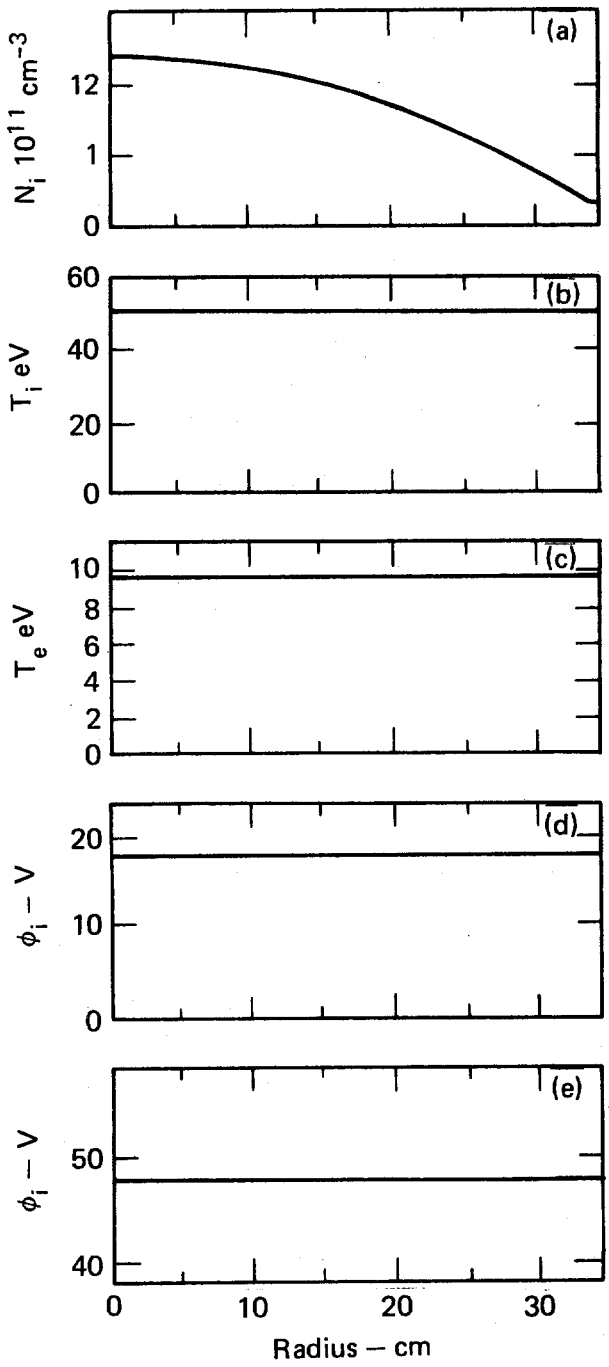

Fig. 1. The radial dependence of the initial center-cell plasma parameters, (t = 0). The plasma parameters are shown as follows:
(a) center cell ion density vs radius,
(b) center cell in temperature vs radius,
(c) electron temperature vs radius,
(d) confining ion potential, ϕ_i, vs radius,
(e) center cell potential, ϕ_e, vs radius.

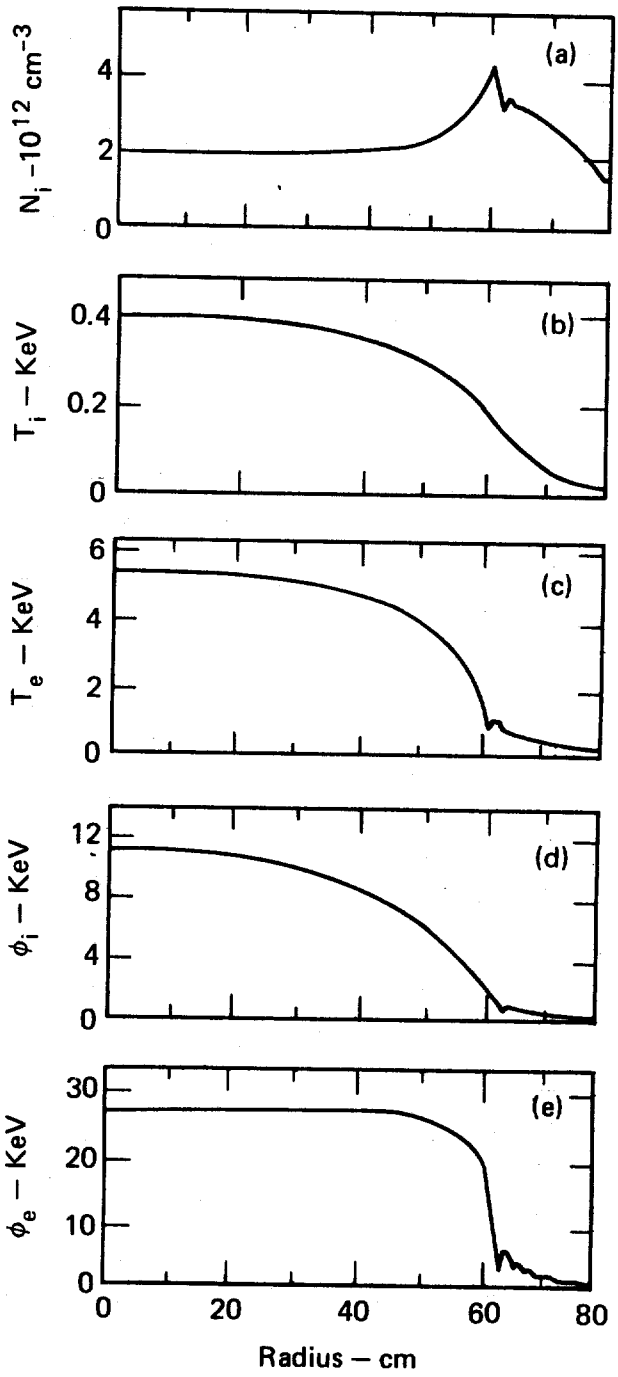

Fig. 2. The radial dependence of the center-cell plasma parameters at time t = 0.5 s for case MF01. The input parameters for this case are summarized in Table IV. These plots show the status at the time the buildup beams are turned off.

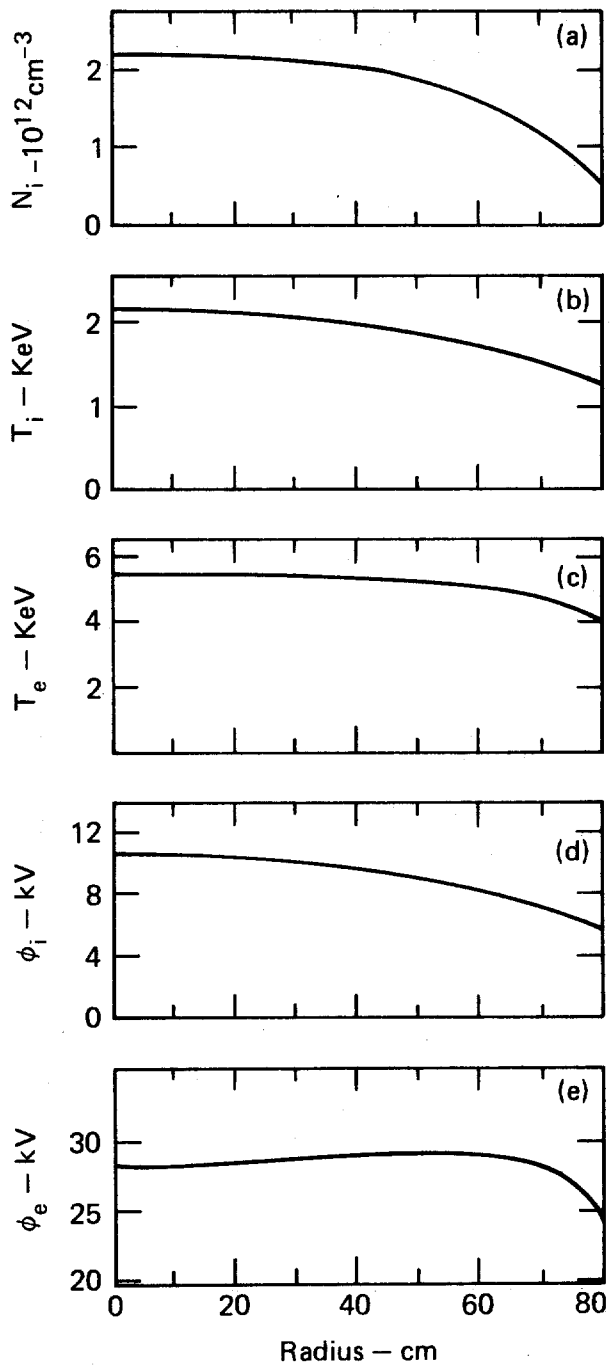

Fig. 3. The radial dependence of the center-cell plasma parameters at time t = 15 s for case MF01. These represent the equilibrium that was achieved.

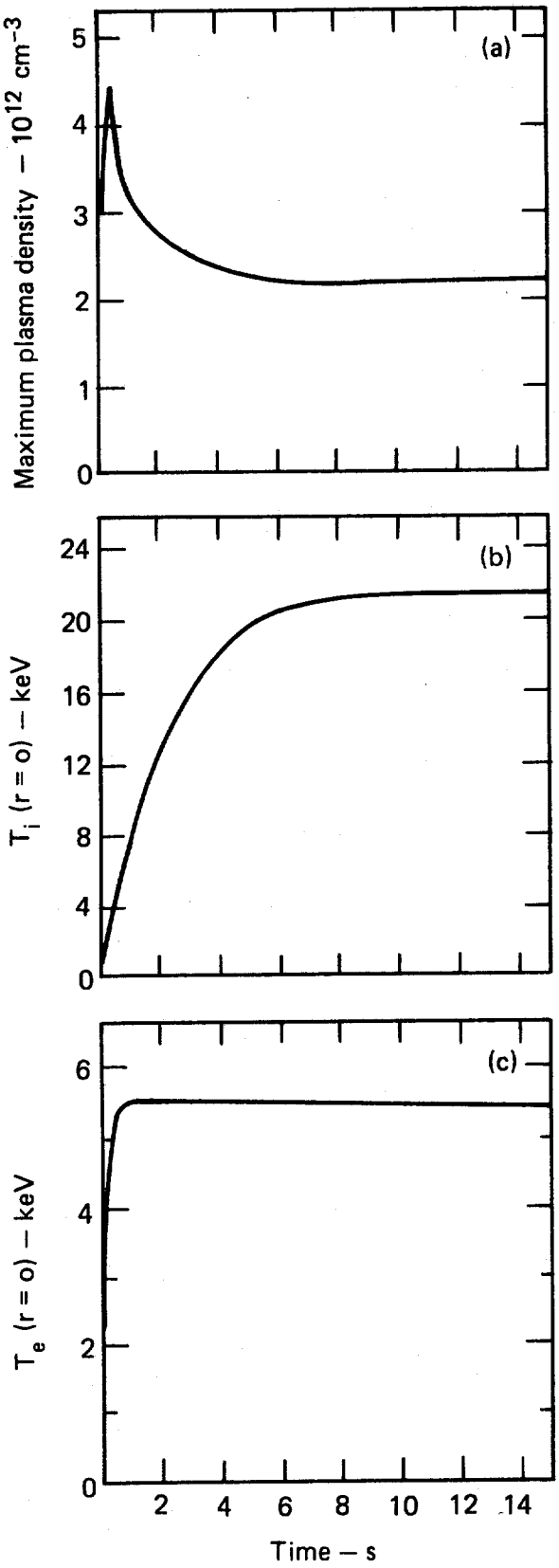

Fig. 4. The time dependence of the maximum center-cell plasma density, the center-cell ion temperature, and the electron temperature for case MF01.

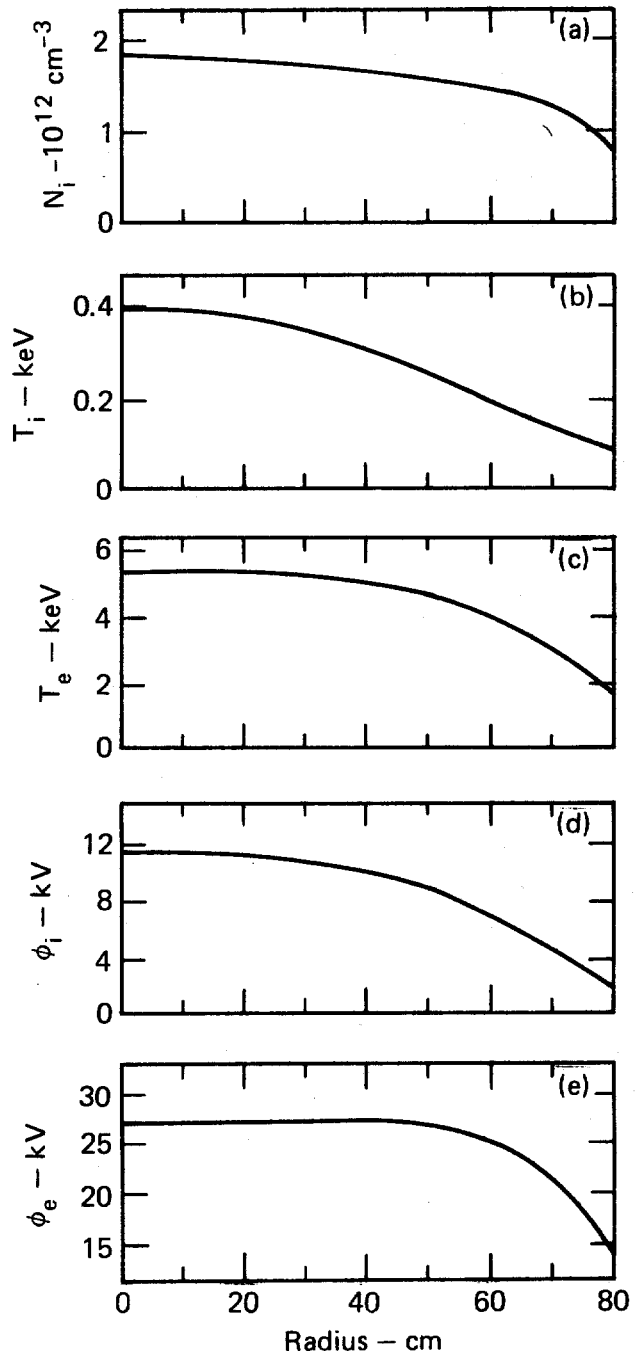

Fig. 5. The radial dependence of the center-cell plasma parameters at time t = 0.5 s for case MF02. The input parameters for this case are summarized in Table IV. These plots show the status at the time the buildup beams are turned off.

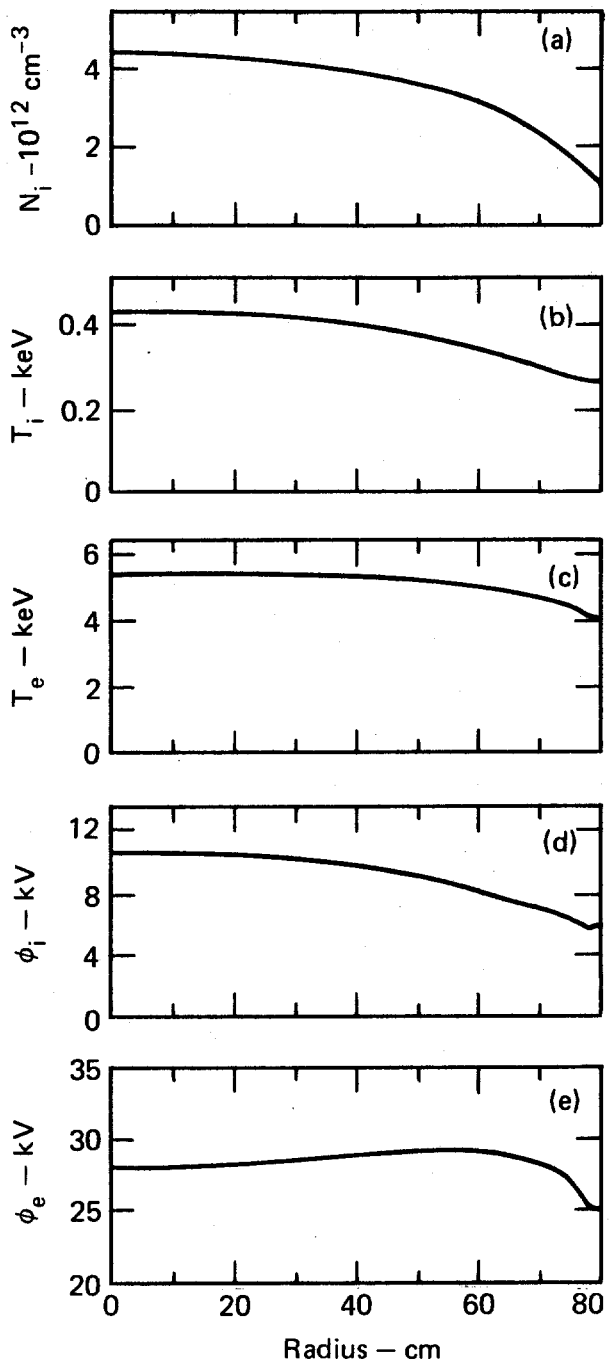

Fig. 6. The radial dependence of the center-cell plasma parameters at time t = 15 s for case MF02. These represent the equilibrium that was achieved.

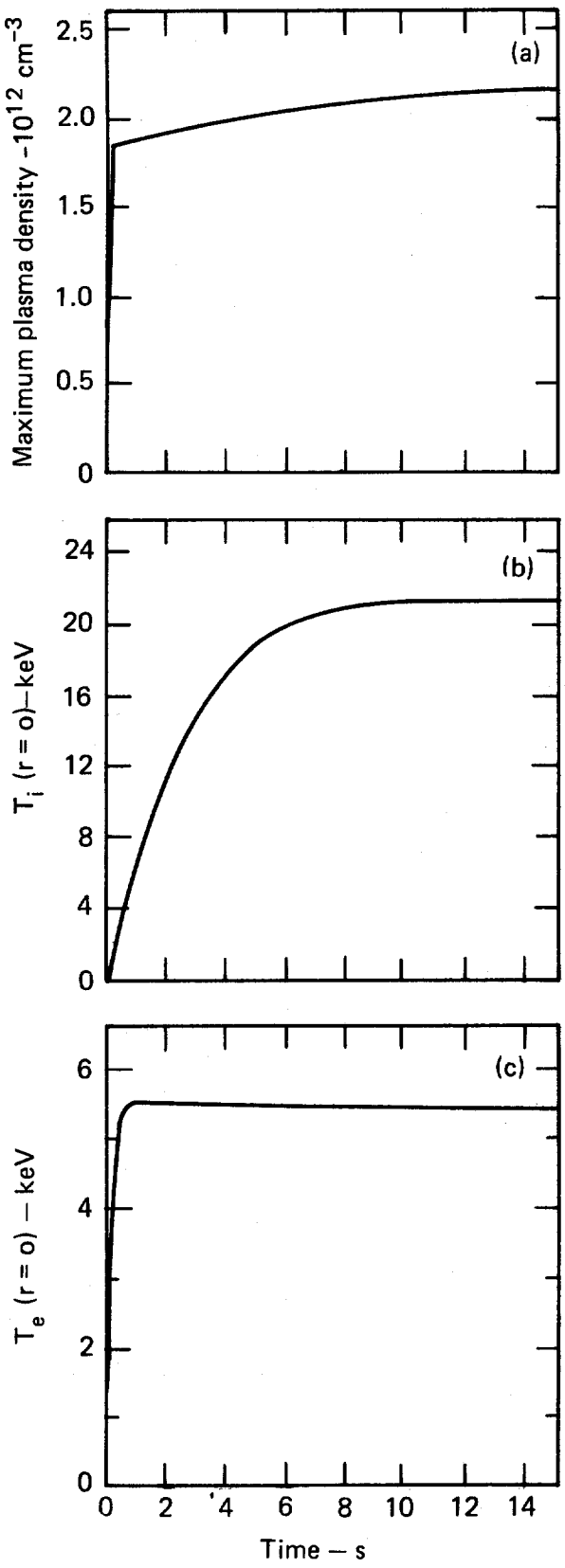

Fig. 7. The time dependence of the maximum center-cell plasma density, the center-cell ion temperature, and the electron temperature for case MF02.

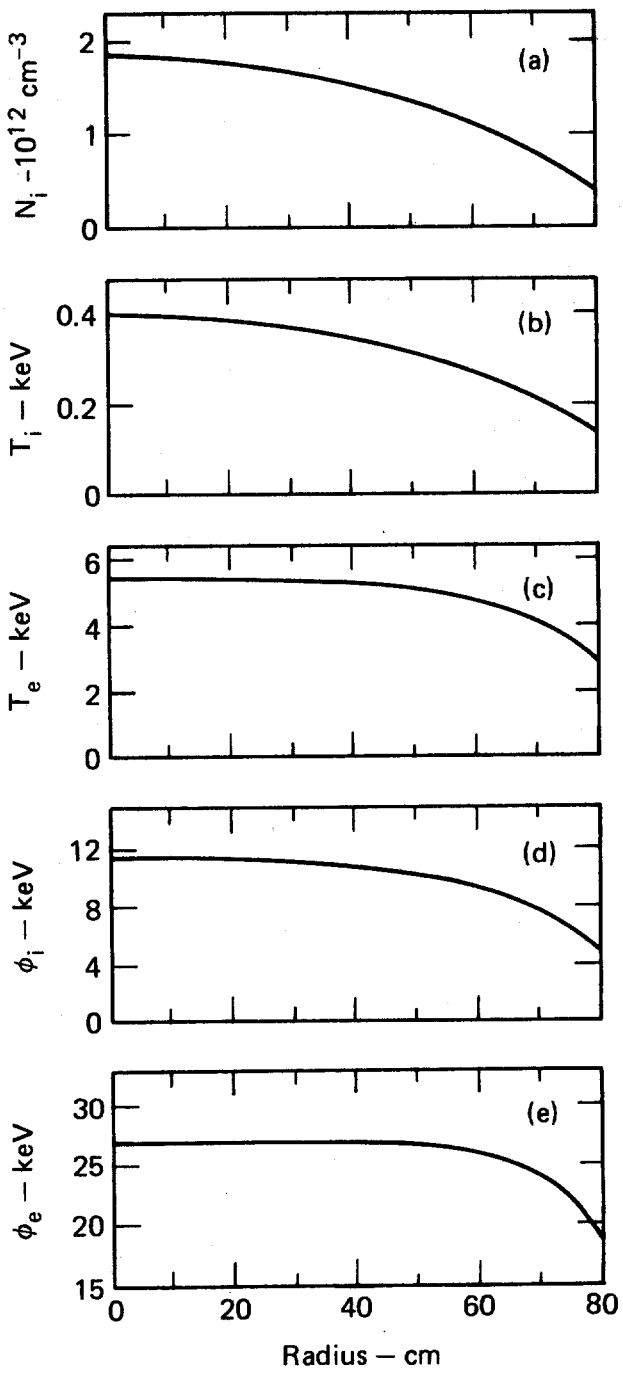

Fig. 8. The radial dependence of the center-cell plasma parameters at time t = 0.5 s for the case MF03. The input parameters for this case are summarized in Table IV. These plots show the status at the time the buildup beams are turned off.

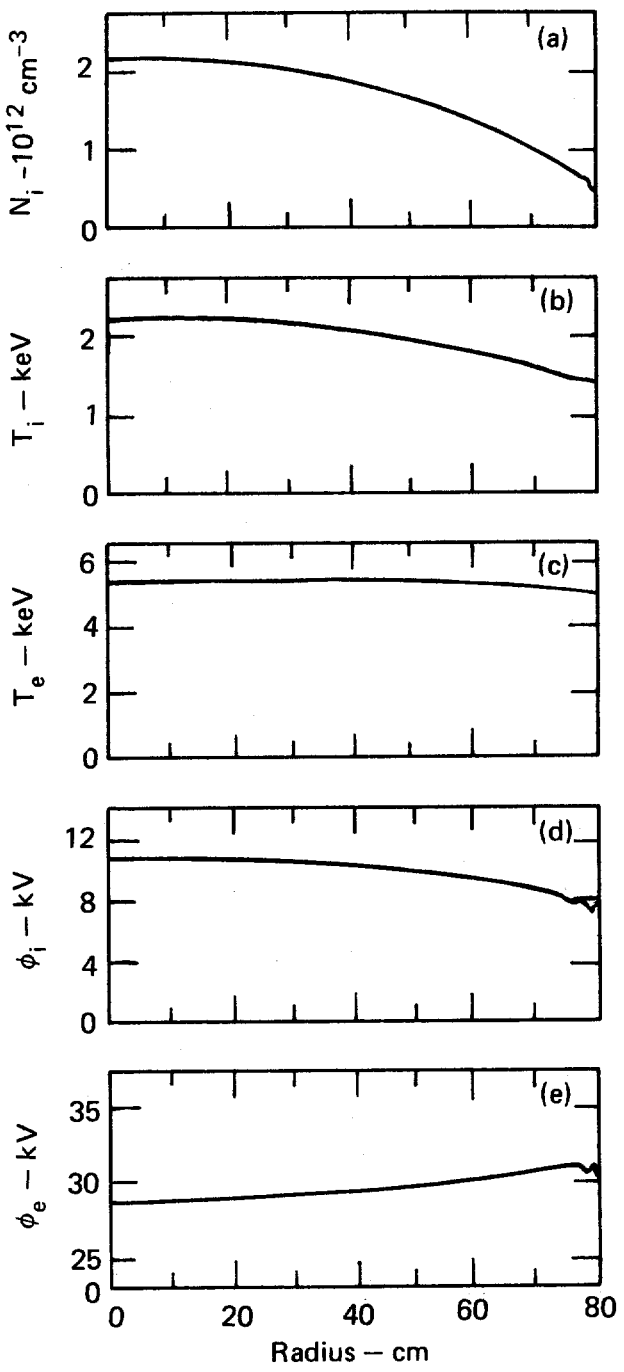

Fig. 9. The radial dependence of the center-cell plasma parameters at time t = 15 s for case MF03. These represent the equilibrium that was achieved.

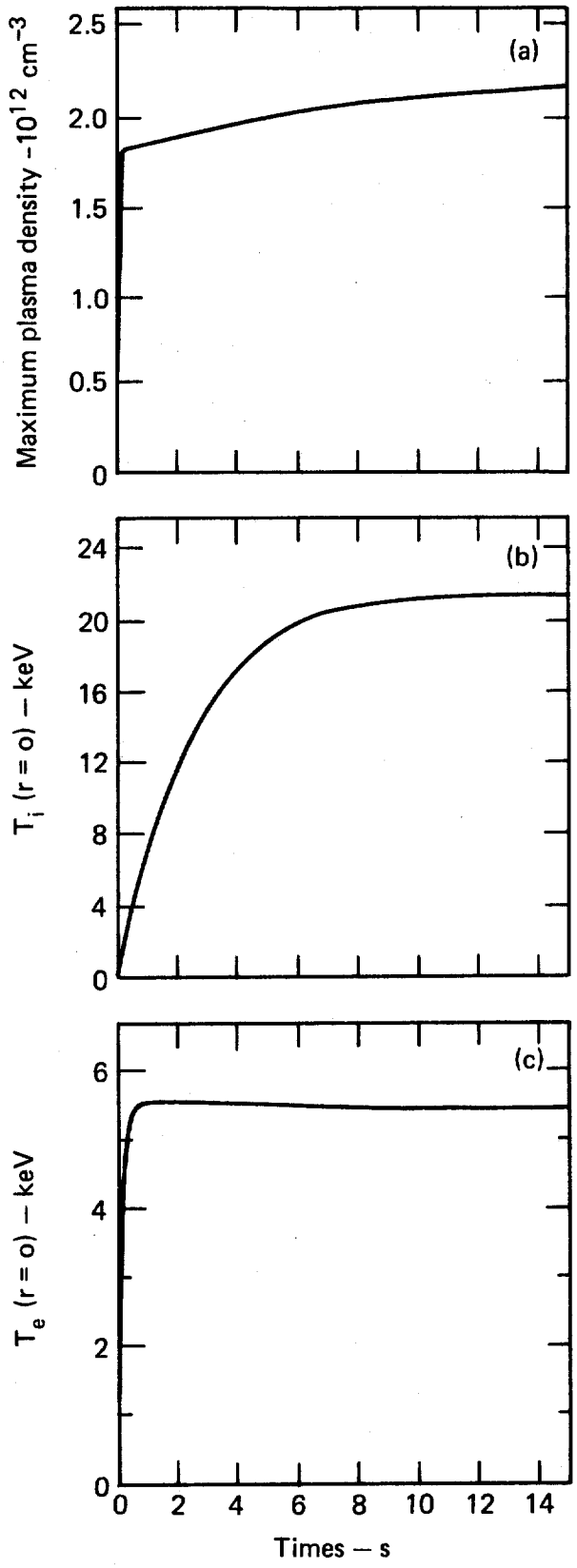

Fig. 10. The time dependence of the maximum center-cell plasma density, the center-cell ion temperature, and the electron temperature for case MF03.

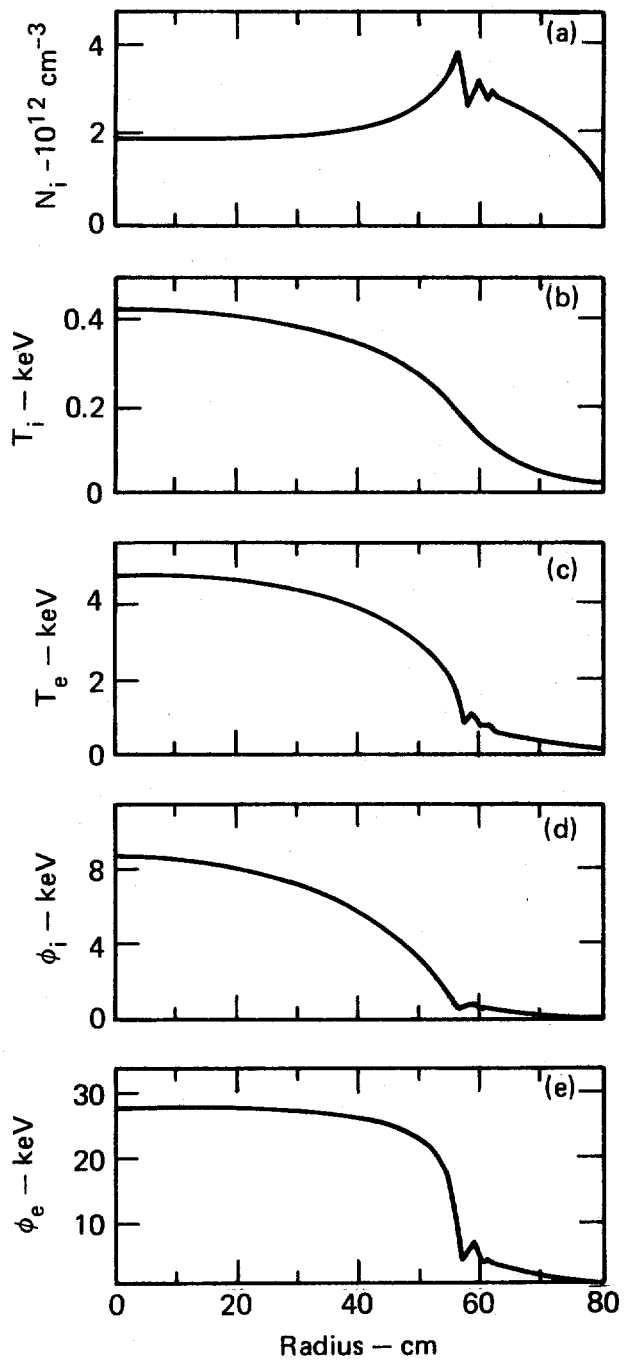

Fig. 11. The radial dependence of the center-cell plasma parameters at time t = 0.5 s for case MF04. The input parameters for this case are summarized in Table IV. These plots show the status at the time the buildup beams are turned off.

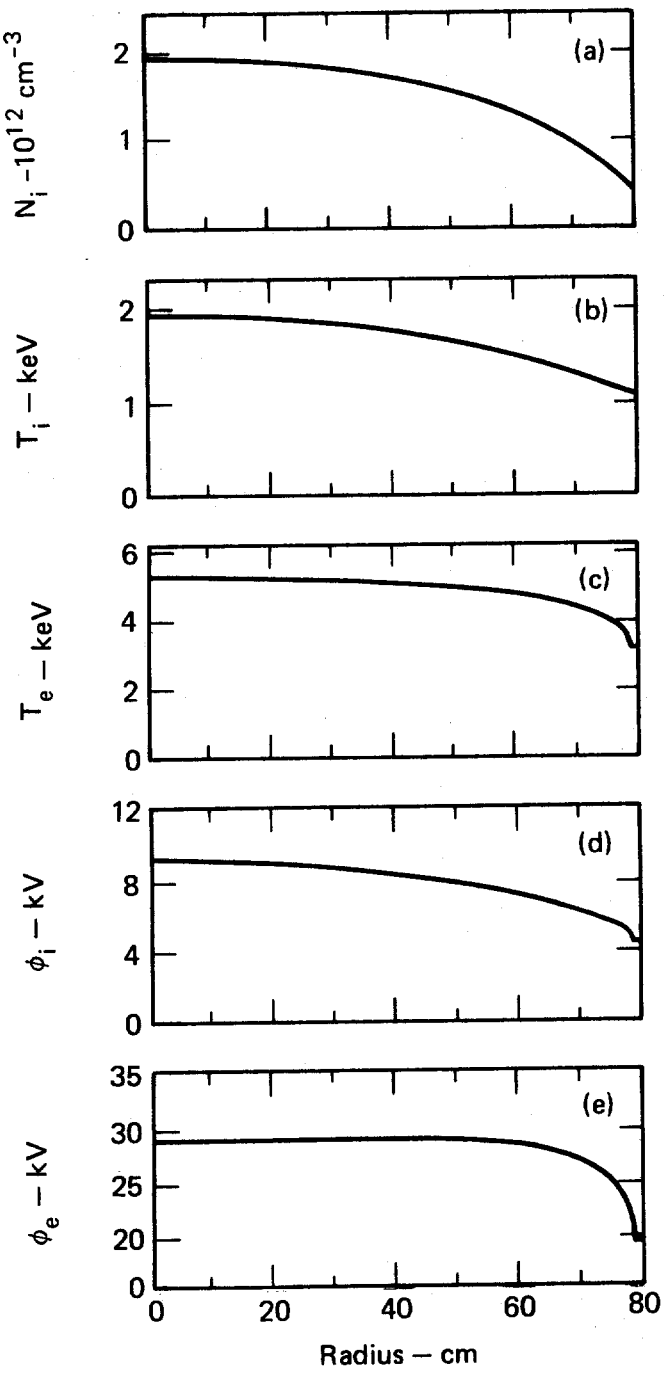

Fig. 12. The radial dependence of the center-cell plasma parameters at time t = 15 s for case MF04. These represent the equilibrium that was achieved.

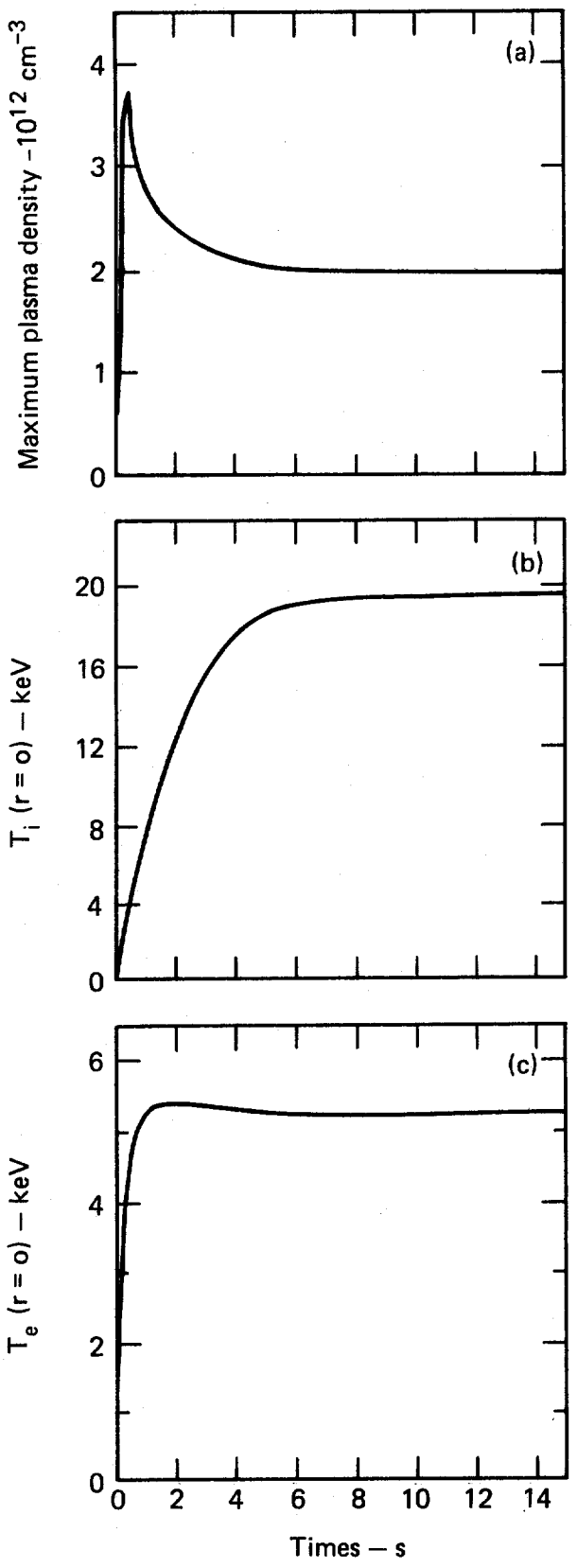

Fig. 13. The time dependence of the maximum center-cell plasma density, the center cell ion temperature, and the electron temperature for case MF04.

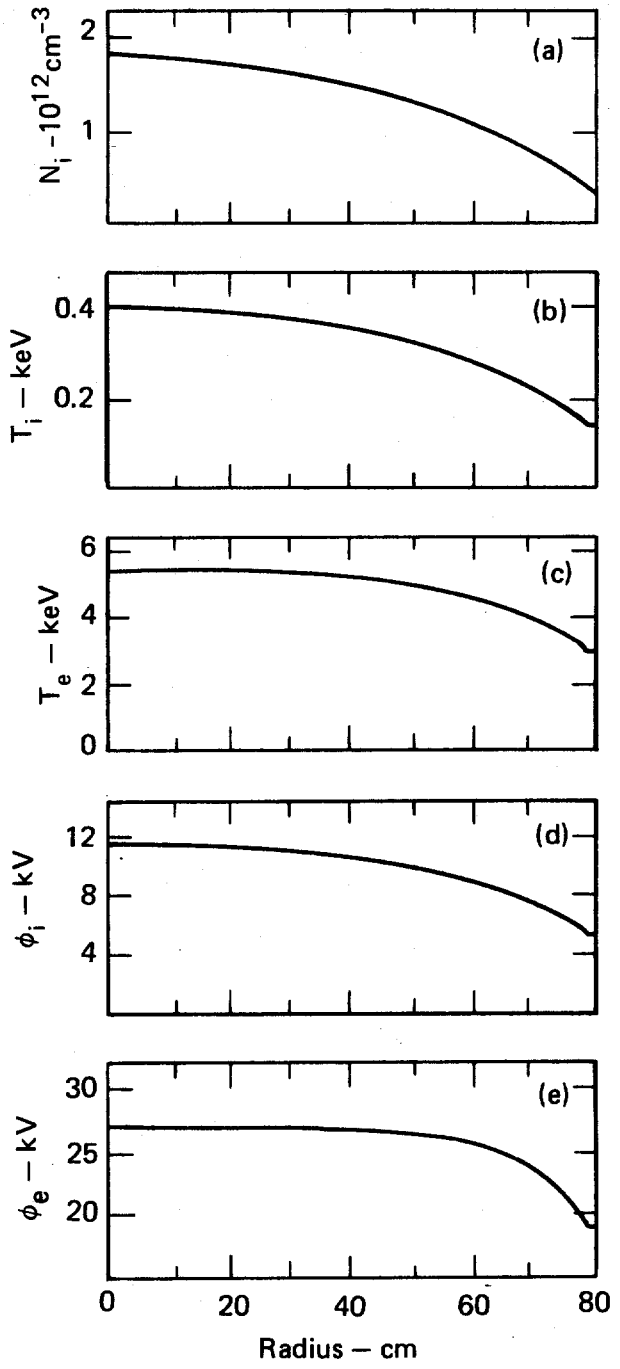

Fig. 14. The radial dependence of the center-cell plasma parameters at time t = 0.5 s for case MF05. The input parameters for this case are summarized in Table IV. These plots show the status at the time the buildup beams are turned off.

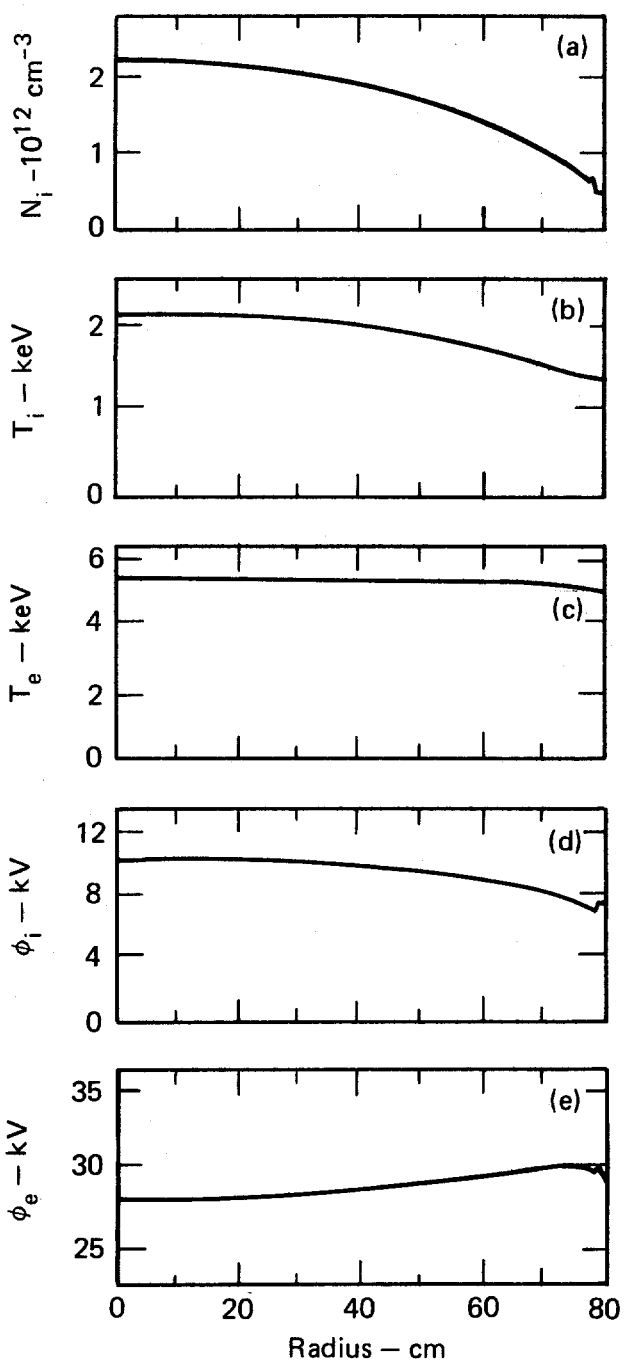

Fig. 15. The radial dependence of the center-cell plasma parameters at time t = 15 s for case MF05. These represent the equilibrium that was achieved.

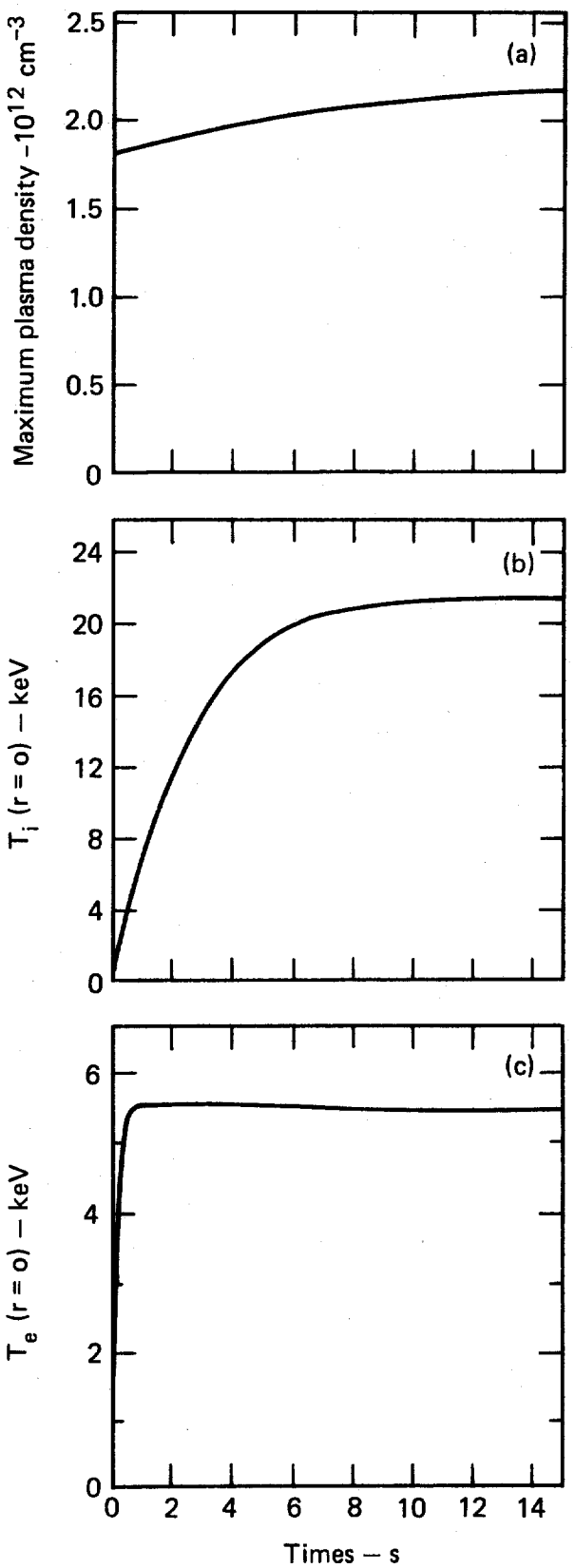

Fig. 16. The time dependence of the maximum center-cell plasma density, the center-cell ion temperature, and the electron temperature for case MF05.

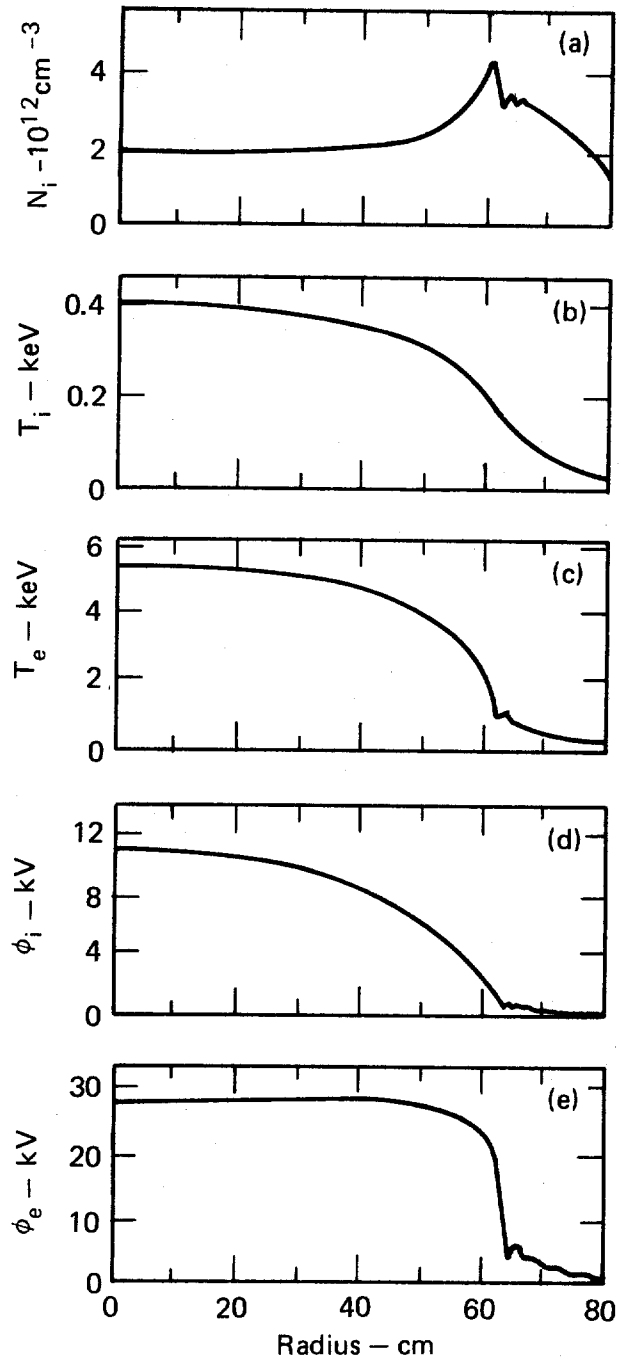

Fig. 17. The radial dependence of the center-cell plasma parameters at time t = 0.5 s for case MF06. The input parameters for this case are summarized in Table IV. These plots show the status at the time the buildup beams are turned off.

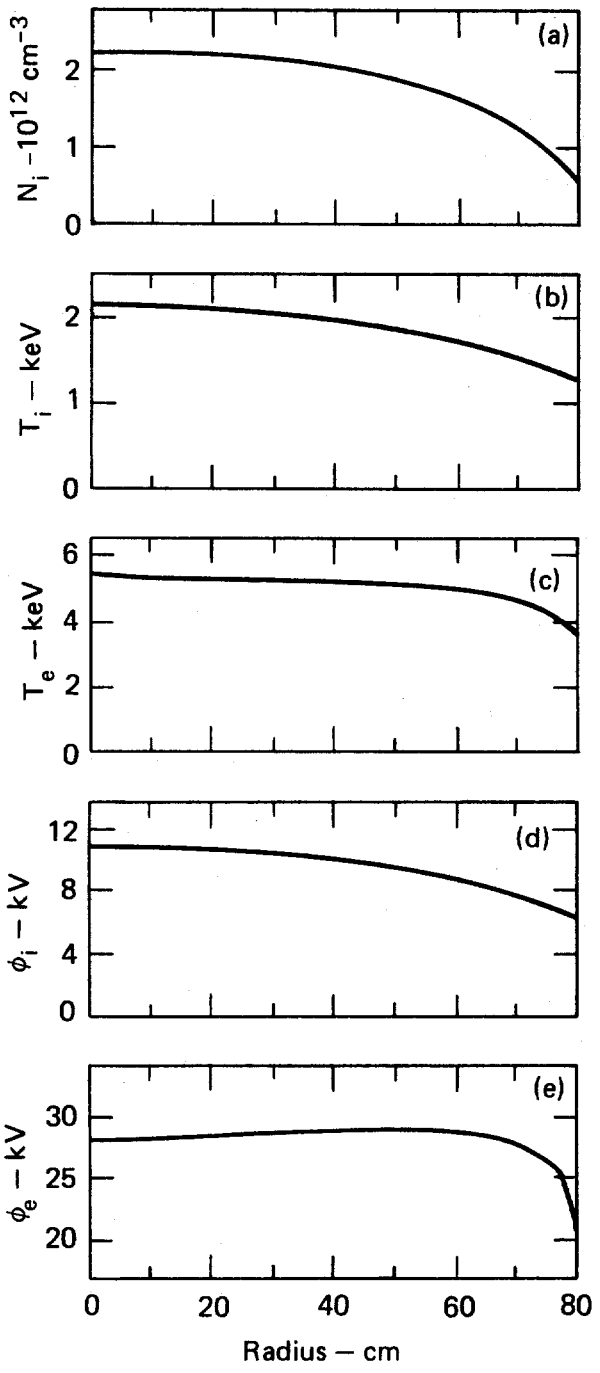

Fig. 18. The radial dependence of the center-cell plasma parameters at time t = 15 s for case MF06. These represent the equilibrium that was achieved.

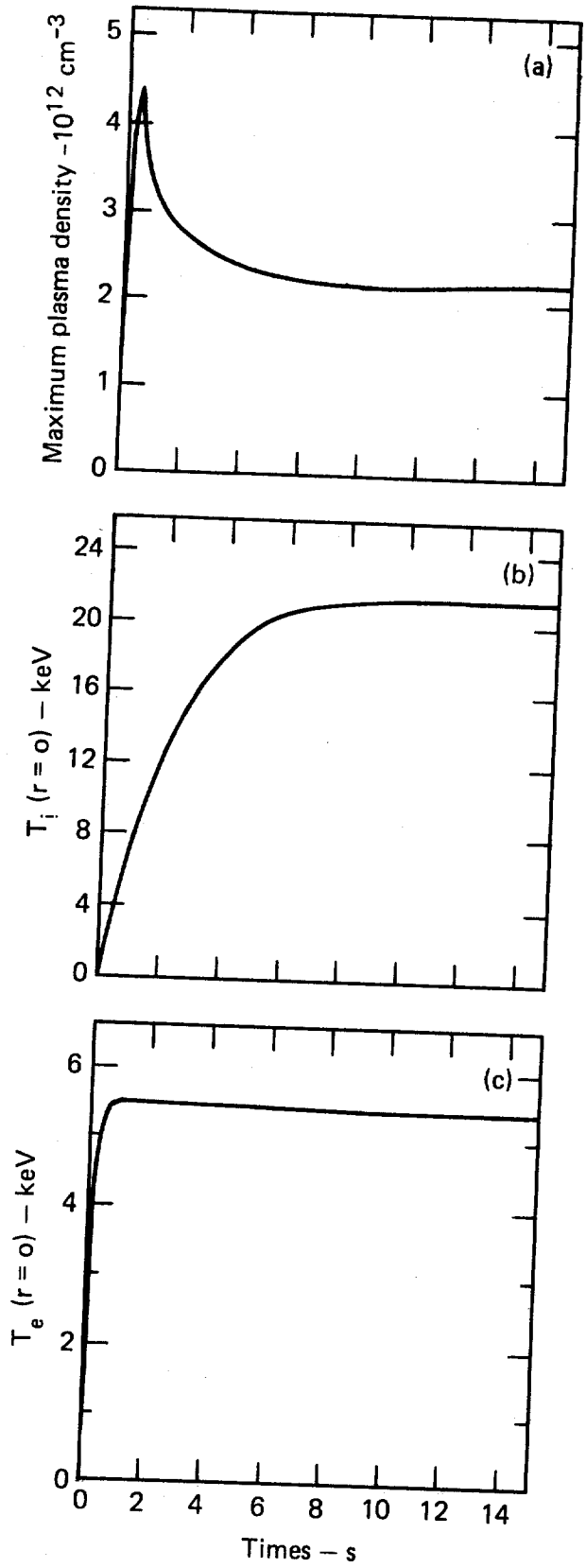

Fig. 19. The time dependence of the maximum center-cell plasma density, the center-cell ion temperature, and the electron temperature for case MF06.

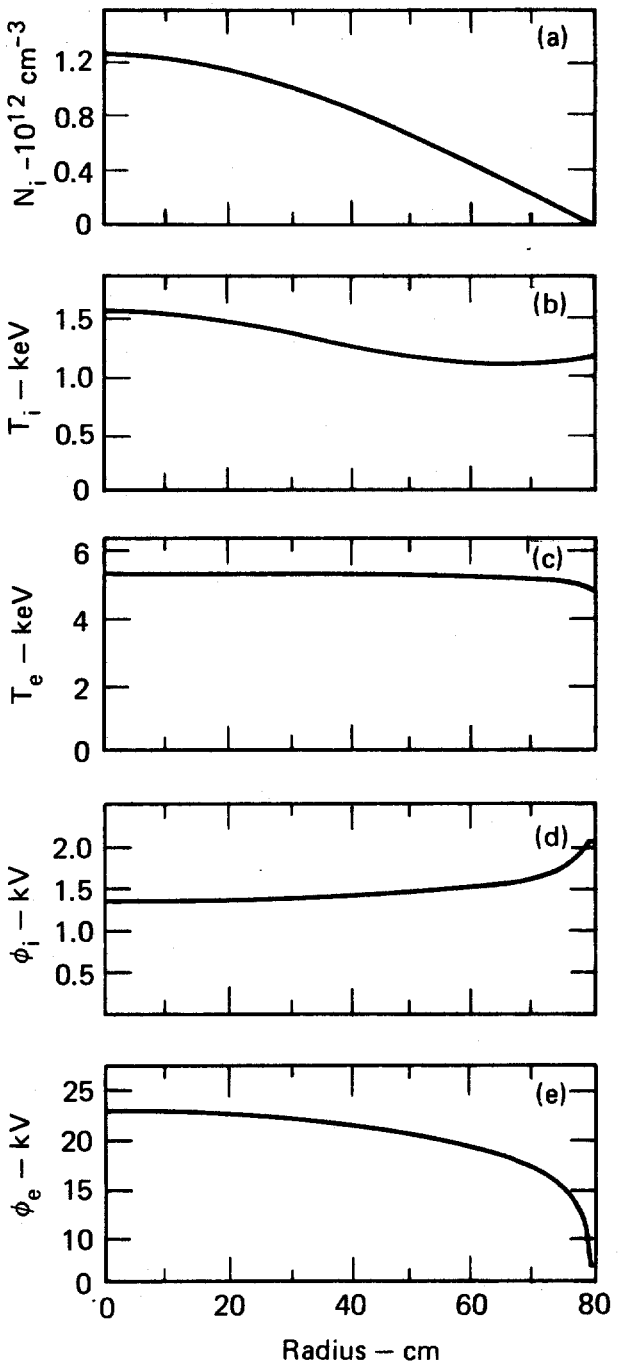

Fig. 20. The equilibrium center-cell plasma parameters for case MF08A (t = 10 s). This case is the same as case MF06 with neo-classical plateau resonant transport. The effect of this transport can be seen by comparing this figure with Fig. 18.

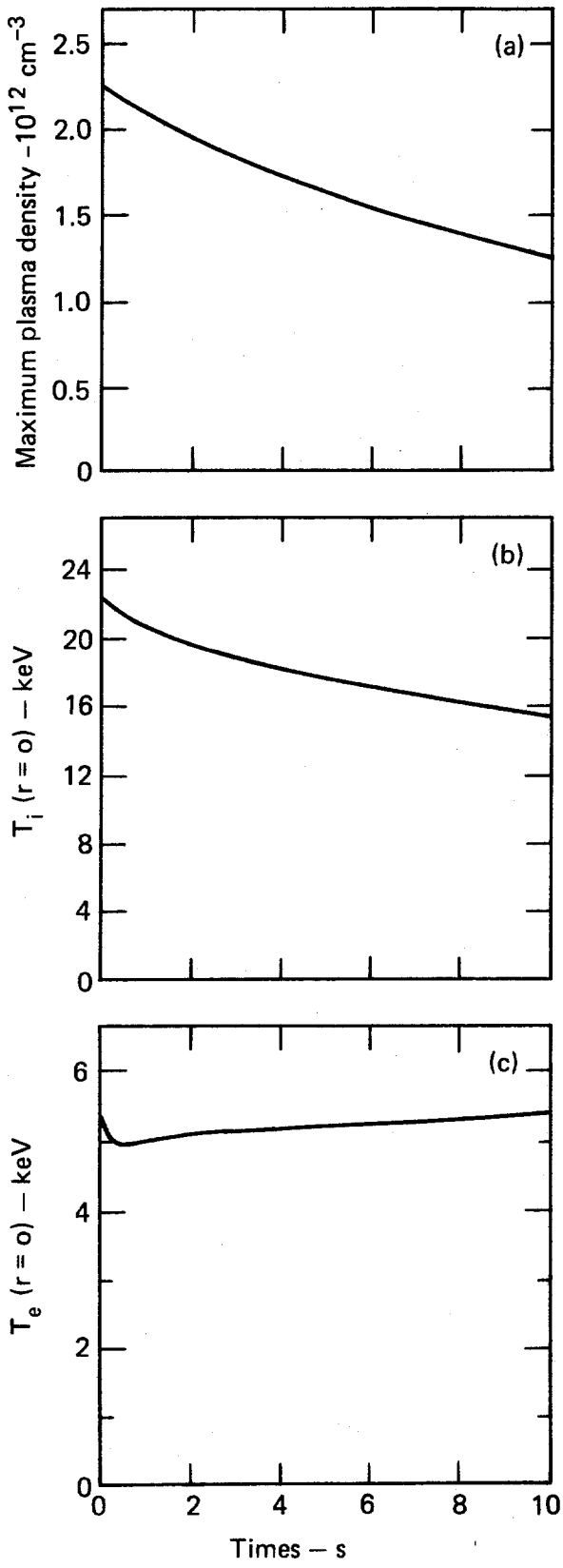

Fig. 21. The time dependence of the maximum center-cell plasma density, the center-cell ion temperature, and the electron temperature for case MF08A.

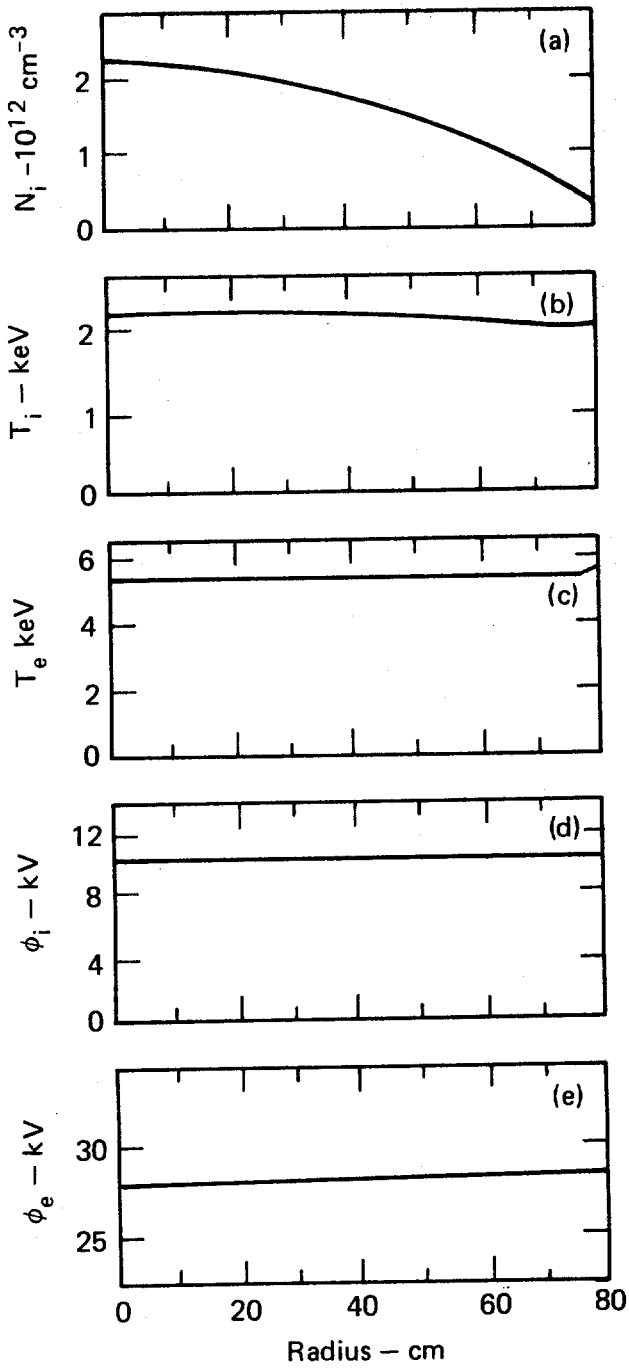

Fig. 22. The equilibrium center cell plasma parameters for case MF09 (t = 1.0 s). This case is the same as case MF06 with classical transport effects. The effect of transport can be seen by comparing this figure with Fig. 18.

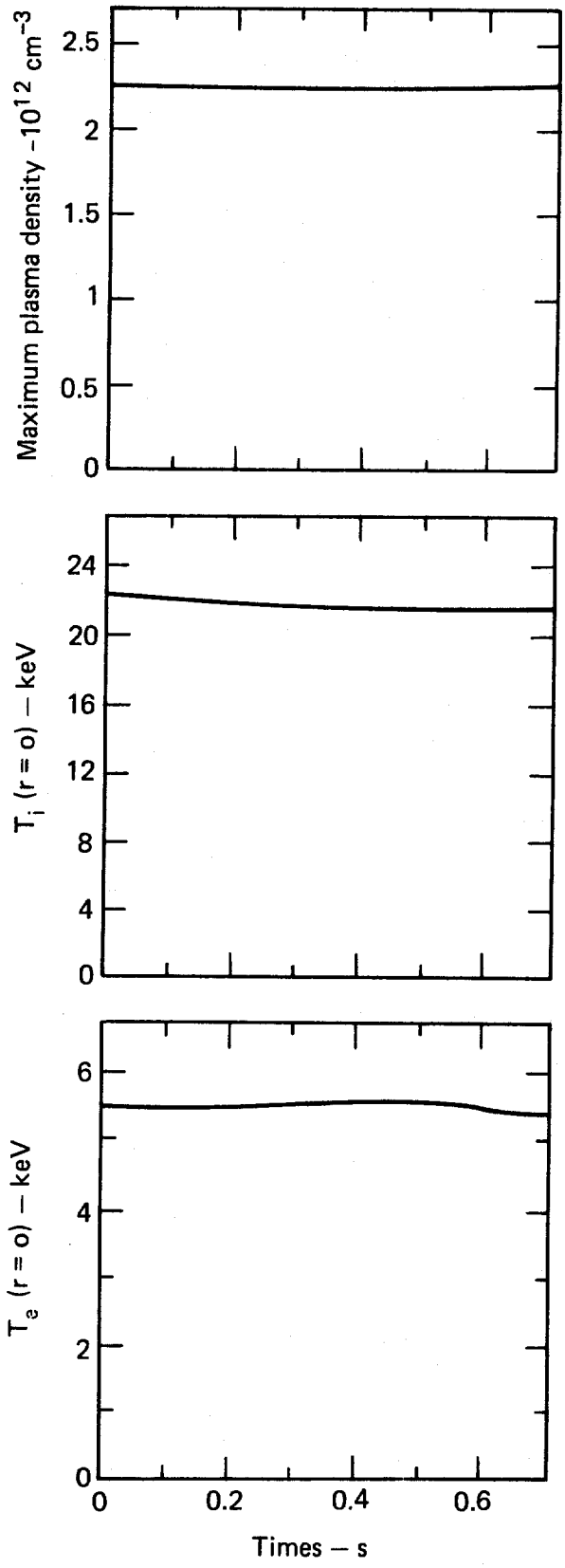

Fig. 23. The time dependence of the maximum center-cell plasma density, the center-cell ion temperature, and the electron temperature for case MF09.

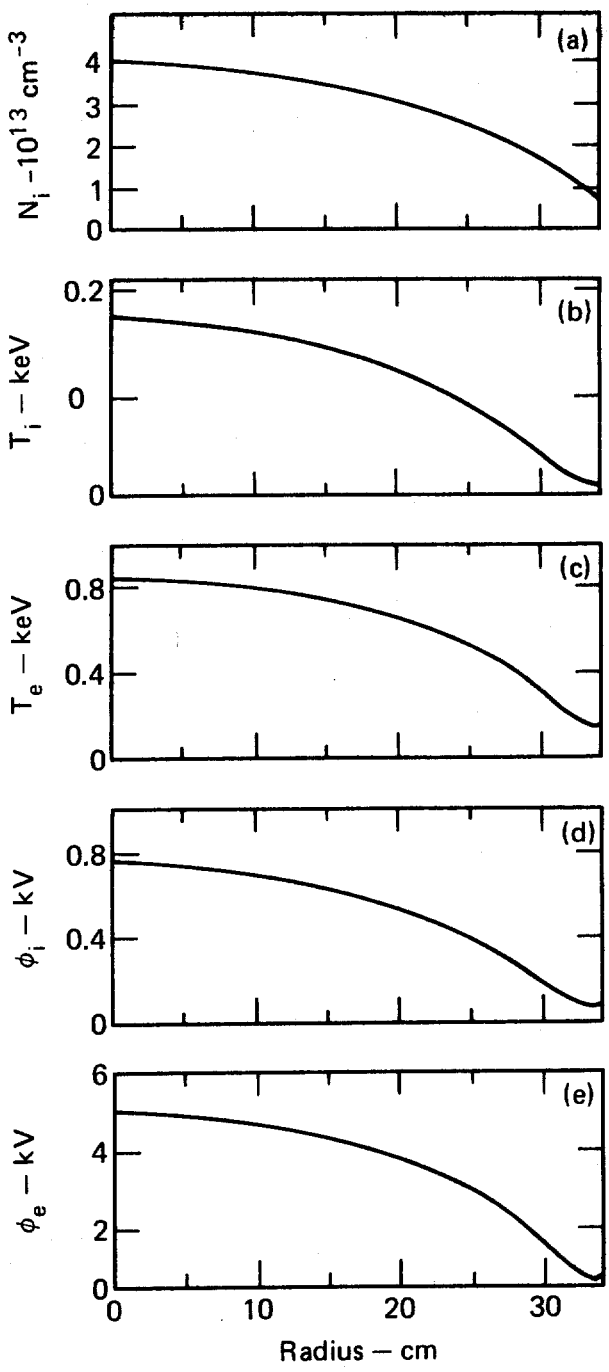

Fig. 24. The radial dependence of the center-cell plasma parameters at time t = 0.5 s for case MF11. This case simulates the two-component operating mode. The input parameters are summarized in Table IV.

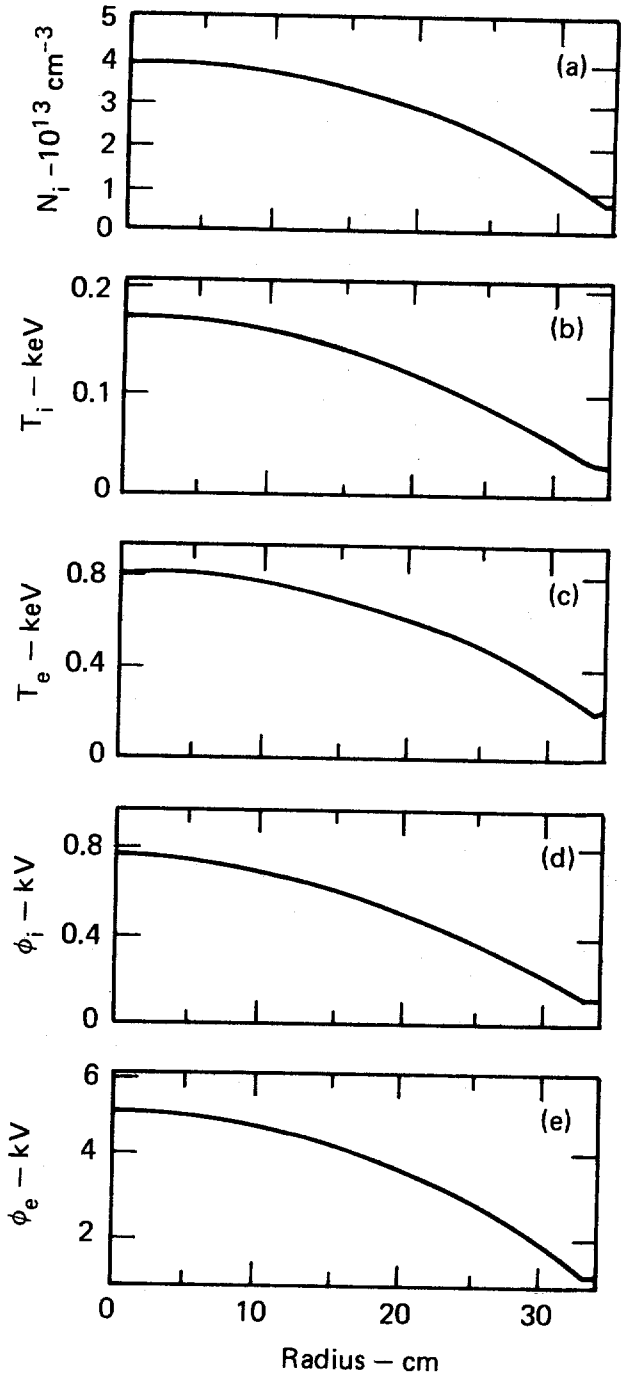

Fig. 25. The radial dependence of the center-cell plasma parameters at time t = 0.8 s for case MF11.

The cases MF08A and MF09 are concerned with the effects of neo-classical, plateau-resonant transport upon the equilibria achieved in the other cases, in which only classical transport was present. The equilibrium densities and temperatures of the MF06 case were used to construct a set of initial profiles, which were then allowed to evolve in time. This is the case MF09. One can see, by comparing the results obtained for the cases MF09 and MF08A (the latter being the case with the addition of neo-classical transport), that the neo-classical, plateau-resonant transport may play an important role in determining the equilibrium reached by the central-cell plasma of MFTF-B.

The case MF11 is concerned with the effects of the unpumped neutral gas upon the equilibrium, two-component-mode plasma. It is seen that a higher neutral-gas density is tolerated by this denser plasma than is tolerated by the low-ε-mode plasma.

Table V shows for various cases, how much the neutral gas incident at the plasma edge can be expected to attenuate as it penetrates the plasma. Typical attenuations from the edge of the plasma to the center of the plasma are on the order of 99%.

Finally, plots of the time behavior of the maximum values of the densities and temperatures are included. For those cases, such as MF01, where the cold, high-density-edge plasma develops, the time-behavior plots track the buildup and subsequent decay of this edge plasma. These plots have the exponential behavior predicted by Eqs. (2.2)-(2.4) predicted for the temperatures and expected for an ion source proportional to the ion density.

SECTION IV. CONCLUSION

A buildup study using a radial transport code has been conducted for MFTF-B plasma and machine parameters. The focus of the study has been to determine the effect of the unpumped neutral gas which accompanies the neutral-beam injection upon the central-cell-plasma buildup and equilibrium. The results of the study indicate that a maximum unpumped-gas density of 1.6×10^{9} cm^{-3} (equivalent current of 274 A) will be tolerated for low-ε-mode parameters for the duration of the neutral-beam injection--0.5 s. The same figure for the two-component-mode parameters is 1.6×10^{10} cm^{-3} (1370 A of equivalent current). Furthermore, in order to obtain rapid ion-density buildup and rapid ion-temperature equilibration to the electron

Table V. Neutral Gas Attenuation

MF01:		
Edge - 0 cm	$n_u = 1.6 \times 10^9$ cm^{-3}	
Center - 40 cm	$n_u = 4.31 \times 10^5$ cm^{-3}	t = 0.4 s
Edge - 80 cm	$n_u = 1.08 \times 10^2$ cm^{-3}	
MF02:		
Edge - 0 cm	$n_u = 1.6 \times 10^8$ cm^{-3}	
Center - 40 cm	$n_u = 7.21 \times 10^5$ cm^{-3}	t = 0.4 s
Edge - 80 cm	$n_u = 3.03 \times 10^3$ cm^{-3}	
MF03:		
Edge - 0 cm	$n_u = 1.6 \times 10^6$ cm^{-3}	
Center - 40 cm	$n_u = 1.14 \times 10^4$ cm^{-3}	t = 0.4 s
Edge - 80 cm	$n_u = 7.63 \times 10^1$ cm^{-3}	
MF04:		
Edge - 0 cm	$n_u = 1.6 \times 10^9$ cm^{-3}	
Center - 40 cm	$n_u = 6.72 \times 10^5$ cm^{-3}	t = 0.4 s
Edge - 80 cm	$n_u = 2.62 \times 10^2$ cm^{-3}	
MF05:		
$n_u = 0$		
MF11:		
Equivalent neutral gas densities to produce trapped ion source of magnitude 1.05×10^{15} cm^{-3} s^{-1}:		
$n_s = 6.86 \times 10^9$ cm^{-3}	0 cm	
$n_s = 1.10 \times 10^9$ cm^{-3}	34 cm	
Gas attenuation (unpumped):		
Edge - 0 cm	$n_u = 1.6 \times 10^{10}$ cm^{-3}	
Center 34 cm	$n_u = 0$ cm^{-3}	
Edge - 68 cm	$n_u = 0$ cm^{-3}	

temperature, there must be a buildup scenario for the low-ε mode in which the streaming-neutral-gas density upon which the plasma builds up is initially high (= 1.6×10^{10} cm^{-3}) and is then reduced (=1.6×10^{6} cm^{-3}) to a lower value once desired center line density (=2×10^{12} cm^{-3}) has been achieved.

Preliminary results of runs using rough approximations to neo-classical, plateau-resonant transport coefficients indicate that neo-classical transport may play a role in determining MFTF-B equilibria.

SECTION V. THE TRANSPORT EQUATIONS

Ion Density:

$$\frac{\partial n_i}{\partial t} = \frac{-1}{r} \frac{\alpha}{\partial r} (r\Gamma_i) + S_i \; ; \tag{5.1}$$

$$\Gamma_i = \sum_{k=1}^{3} D_{1k} \frac{\partial u_k}{\partial r} \; . \tag{5.2}$$

Ion Temperature:

$$\frac{\partial T_i}{\partial t} = \frac{-\Gamma i}{n_i} \frac{\partial T_i}{\partial r} - \frac{2}{3} \frac{T_i}{r} \frac{\partial}{\partial r} \left(\frac{r\Gamma_i}{n_i} \right) - \frac{2}{3} \frac{1}{rn_i} \frac{\partial (rq_i)}{\partial r} + \frac{T_e - T_i}{\tau_{ei}} + \frac{T_i S_i}{n_i} \; ; \tag{5.3}$$

$$q_i = \sum_{k=1}^{3} D_{2k} \frac{\partial u_k}{\partial r} \; . \tag{5.4}$$

Electron Density (per unit flux tube):

$$\frac{\partial N}{\partial t} = \frac{-1}{r} \frac{\partial}{\partial r} (r\Gamma_e) + S_e \; , \tag{5.5}$$

where

$$\Gamma_e = L_s \Gamma_i + \frac{2L_p}{R} \sum_{k=1}^{3} D_{4k} \frac{\partial u_k}{\partial r} \tag{5.5}$$

$L_p \equiv$ plug length
$R \equiv$ mirror ratio between middle of central cell and middle of plug;

$$\frac{\partial T_e}{\partial t} = \frac{-\Gamma_e}{N} \frac{\partial T_e}{\partial r} - \frac{2}{3} \frac{T_e}{r} \frac{\partial}{\partial r} \left(\frac{r\Gamma_e}{N} \right) - \frac{2}{3} \frac{1}{Nr} \frac{\partial}{\partial r} (rq_e) + \frac{T_i - T_e}{\tau_{ei}} + \frac{T_e S_e}{N} + \frac{2}{3} \frac{Q_e}{N} , \tag{5.6}$$

where

$$q_e = \sum_{k=1}^{3} D_{3k} \frac{\partial u_k}{\partial r} , \tag{5.7}$$

$$\bar{u} = (n_i, T_i, T_e) . \tag{5.8}$$

The classical contribution to the fluxes is given by:

$$D_{11} = \frac{-\beta}{n} (n_i T_e + n_i T_i) \tag{5.9}$$

$$\beta = (m_e \Omega_e^2 \tau_e)^{-1}$$

$$\Omega_e = \frac{eB_s}{m_e c} \qquad \Omega_i = \frac{eB_s}{m_i c}$$

$$D_{12} = -\beta n_i$$

$$D_{13} = \frac{1}{2} \beta n_i$$

$$D_{14} = 0$$

$$D_{21} = 0 \tag{5.10}$$

$$D_{22} = -2 \beta_i n_i T_i$$

$$\beta_i = (m_i \Omega_i {}^2 \tau_i)^{-1}$$

$$D_{23} = 0 \qquad D_{24} = 0$$

$$D_{31} = 3/2 \ \beta T_e (T_e + T_i) \tag{5.11}$$

$$
\begin{aligned}
D_{32} &= 3/2\ \beta\ T_e\ n_i \\
D_{33} &= -\ 3.16\ \beta\ T_e n_i \\
D_{34} &= 0 \\
D_{41} &= 0 \\
D_{42} &= 0 \\
D_{43} &= 0
\end{aligned}
\tag{5.12}
$$

It should be noted that the classical contribution to the electron flux is ambipolar as given in equation (5.5).

$$
Q_e = \overline{N} \times \overline{Q} \times \overline{N} + Q_{enc} \tag{5.13}
$$

$$
\overline{N} = \left(\frac{\partial n_i}{\partial r} , \frac{\partial T_i}{\partial r} , \frac{\partial T_e}{\partial r} \right)
$$

$$
Q_{11} = -\beta \left(\frac{T_i^{\,2}}{n_i} + T_e \frac{(T_e + 2T_i)}{n_i} \right)
$$

$$
\begin{aligned}
Q_{12} &= -\beta(T_i + T_e) \\
Q_{13} &= \beta/2\ (T_i + T_e) \\
Q_{21} &= -Q_{12} \\
Q_{22} &= n_i \beta \\
Q_{23} &= -1/2\ \beta_i n_i \\
Q_{31} &= \beta(T_e + T_i) \\
Q_{32} &= \beta n_i \\
Q_{33} &= -1/2\ \beta n_i \\
Q_{enc} &= \text{neo-classical contribution to heat generation in the electrons, defined subsequently.}
\end{aligned}
$$

The relaxation times are:

self,

$$
\tau_j = \frac{3\sqrt{m_j}}{4\sqrt{\pi}} \frac{(kT_j)^{3/2}}{\lambda_{jj}\ e^4\ n_j} \quad ; \tag{5.14}
$$

exchange,

$$\tau_{jk} = \frac{3}{9\sqrt{2\pi}} \frac{m_j m_k}{\lambda_{jk} e^4 n_k} \left(\frac{kT_j}{m_j} + \frac{kT_k}{m_k} \right)^{3/2} \frac{1}{Z_j^2 Z_k^2} \quad , \tag{5.15}$$

with T_j in K.

The neo-classical plateau resonant transport contribution to the fluxes is given by:

$$D_{11} = - \frac{\sqrt{\pi}}{2} \left(\frac{kT_i}{m_i} \right)^{3/2} \left(\frac{r_c}{L_{tr}} \frac{1}{\Omega_i} \right)^{3/2} \frac{1}{L_s} \quad , \tag{5.16}$$

where

$r_c \equiv$ radius of central cell plasma
$L_s \equiv$ length of central cell plasma
$L_{tr} \equiv$ length of quadrupole transition region = 700 cm for MFTF-B

$$\begin{aligned} D_{12} &= D_{13} = D_{14} = 0 \\ D_{21} &= D_{23} = D_{24} = 0 \\ D_{22} &= D_{11} n_i \end{aligned} \tag{5.17}$$

$$D_{31} = D_{32} = D_{34} = 0 \tag{5.18}$$

$$D_{33} = - \left[(r_p^2 / L_{tr} / L_{p\ 1/2})\ Te \left\{ \left(T_e + \frac{\phi_i}{R_p - 1} \right)^{-1} - \left(T_e + \frac{\phi_m}{R_p - 1} \right)^{-1} \right\}^2 \right] \times r_p^2 \nu_{eep} n_p \frac{2L_p}{R}$$

where

ν_{eep} ≡ electron self-relaxation frequency in plug in s^{-1}

r_p ≡ radius of plug plasma

$L_{p\ 1/2}$ ≡ half-length of plug

$\phi_m \equiv \phi_i + \phi_e$

R_p ≡ plug mirror ratio.

$$D_{41} = (D_{33}/n_p)\ (\partial n_p/\partial r)/(\partial n_i/\partial r) \tag{5.19}$$

$$D_{42} = D_{43} = D_{44} = 0$$

$$Q_{enc} = (D_{33}/np)(2Lp/R)(\partial\phi/\partial r)(\partial np/\partial r) \tag{5.20}$$

The values of the neo-classical transport coefficients are computed on the center line ($r = 0$) at each time step and then fixed at this center line value for all other values of $r > 0$.

The source terms in equations (5.1), (5.3), (5.5), and (5.6) contain contributions to the time evolution of the densities and temperatures from charge exchange, ionization, recombination, etc. In addition, these terms include the Pastukhov end-loss expressions for axial particle and energy loss given in detail in Refs. 1 and 6:

$$\tau_p\ (j, \phi, \zeta, p) = \tau_j \frac{\pi^{1/2}}{4} \ln \frac{(4\zeta\rho + 2)}{\zeta} \frac{z_j\phi}{T_j} \left(\frac{2\zeta\rho + 1}{2\zeta\rho}\right) x \exp \frac{z_j\phi}{T_j} \frac{1}{I(T_j/z_j\phi)} \tag{5.21}$$

$$\tau_j = \frac{m_j^{1/2}\ T_j^{3/2}}{\sqrt{2\pi}\ e^4 z_j^2 \sum_k \lambda_{jk}\ n_k\ z_k^2} \tag{5.22}$$

$$I(X) \cong \frac{1 + X/2}{1 + X^2/4}, \tag{5.23}$$

where

$$\left(\frac{dn_i}{dt}\right)_{E1} = \frac{-n_i}{\tau} \tag{5.24}$$

$$\tau = \tau_p(i,\ \phi_i,\ z_i,\ R).$$

$$\left(\frac{dT_i}{dt}\right)_{E1} = \frac{-\frac{2}{3}\, z\ e\phi_i}{I(T_i/z_i\phi_i)}\ \frac{1}{\tau} \tag{5.25}$$

$$\left(\frac{dT_e}{dt}\right)_{E1} = \frac{-N_{ep}}{N}\ \frac{1}{\langle\tau\rangle}\ \frac{\phi_i + \phi_e}{I\ \frac{T_e}{(\phi_i + \phi_e)}} \tag{5.26}$$

where

$$N_{ep} = \frac{2L_p}{R}\ n_p\ .$$

$$\left(\frac{dN}{dt}\right)_{E1} = \frac{-N_{ep}}{\langle\tau\rangle} \tag{5.27}$$

$$\langle\tau\rangle \equiv \tau_p(e,\ \phi_i + \phi_e,\ \langle z\rangle,\ R_p \tag{5.28}$$

$$\tau_e = m_e^{1/2} m\ \tau_e^{3/2}/(\sqrt{2}\,\pi\ e^4\ n_p\ \lambda_{eep}\ \langle\varepsilon\rangle) \tag{5.29}$$

$$\langle\varepsilon\rangle = 1 + \frac{L_s}{2L_p}\ \frac{\lambda_{ess}}{\lambda_{eep}}\ \frac{n_i}{n_p}\ \frac{\phi_i + \phi_e}{\phi_e} \tag{5.30}$$

$$\langle z\rangle = \frac{\zeta_p + \frac{N_{es}}{N_{ep}}\ \frac{\phi_i + \phi_e}{e}\ \frac{\lambda_{ees}}{eep}\ \zeta c}{1 + \frac{n_i}{n_p}\ \frac{\phi_i + \phi_e}{\phi_e}\ \frac{L_s}{2L_p}\ \frac{\lambda_{ees}}{\lambda_{eep}}} \tag{5.31}$$

where

$$N_{es} = L_s n_i .$$

$$\zeta_c = \frac{1}{2}\left[1 + \frac{1}{n_i} \sum_{\substack{\text{solenoid} \\ \text{ions}}} n_j z_j^2 \frac{\lambda_{ej}}{\lambda_{ess}}\right] \tag{5.32}$$

where the subscript s refers to central cell and p refers to plug. Equation (5.31) gives ζ_p with the sum being over plug ions and λ_{ees} replaced by λ_{eep}.

SECTION VI. NEUTRAL GAS EQUATIONS

The equations which are used to solve for the radial dependence of the unpumped-neutral-gas density are:

$$v_G \frac{\partial n_G}{\partial x} = - \beta_G n_G \tag{6.1}$$

$$\beta_G = n_i \left\langle \sigma^i_{IG} \; v_{iG} \right\rangle + n_i \left\langle \sigma^e_{IG} \; v_{eG} \right\rangle + n_i \left\langle \sigma^i_{cxG} \; v_{iG} \right\rangle . \tag{6.2}$$

These equations are solved subject to the boundary condition

$$n_G \; (x = r_c) = n_{Go} \tag{6.3}$$

$n_{Go} \equiv$ neutral gas density incident upon the plasma at its edge.

The terms included in equation (6.2) represent neutral loss due to electron and ion impact ionization and charge exchange. The latter term is included in order to be consistent with the previously stated assumption that all charge exchange reactions with the virgin, non-reacted, neutral gas result in the birth of a hot neutral which is immediately lost from the plasma. If the approximation is made that the ion densities and $\langle \sigma v \rangle$ values are slowly varying across the plasma (from mesh point to mesh point in code terminology) the Eq. (6.1) can be immedately integrated.

$$n_G(x_j + 1) = n_G(x_j)\exp\ -\alpha_G(x_j + 1) - x_j\ ; \tag{6.4}$$

$$\alpha_G = \frac{\bar{\beta}G}{v_G}$$

$$\bar{\beta}_G = \frac{1}{2}\left[\beta_G\ (x_j + 1) + \beta_G\ (x_j)\right]\ , \tag{6.5}$$

where $j = (-n + 1), \ldots, 0, \ldots n$ with $x_{(-n = 1)} \equiv r_c$, $x_n \equiv 2r_c$. The further approximation that the neutral gas is a beam of width $W_B = r_c$ now yields[8]:

$$\tilde{n}_G(r) = \frac{1}{2\pi}\int_{-\pi/2}^{\pi/2} d\theta H\left[W_B{}^2 - r^2\ \sin^2\theta\right]\ n_G(r\ \cos\theta) \tag{6.6}$$

$$\begin{aligned} H(\xi) &= 1; \qquad \xi \geq 0 \\ H(\xi) &= 0; \qquad \xi < 0 \end{aligned} \tag{6.7}$$

Performing the integration indicated in Eq. (6.6) then gives[8]:

$$\tilde{n}_G(r) = \left[n_G(-r) + n_G(r)\right]\ \frac{1}{2\pi}\ \sin\frac{-1y}{r}\Bigg|_{\max\ (-r,\ W_B)}^{\min\ (r,\ W_B)} \qquad r\ \cos\theta \to \pm\sqrt{r^2}\ . \tag{6.8}$$

This result summarizes the azimuthal averaging used for the case when the finite-Larmor-radius corrections are not included. The inclusion of the FLR corrections yields more complicated results. Since these corrections are not significant for the cold-gas-feed model being utilized, they will not be discussed.

SECTION VII. METHOD OF SOLUTION FOR ϕ_e

The problem of solving for the potential, ϕ_e, as outlined in Eq. (1.5) can be reduced to the problem

$$\frac{Gw(X)}{X} e^{-X} = c_w(X) \tag{7.1}$$

$$X = \frac{\phi_i + \phi_e}{T_e} , \tag{7.2}$$

where $\lim_{X \to 0} \frac{Gw(X)}{X} = \tau_{MC}$ (τ_{MC} is the classical mirror loss time).

Gw(X) and Cw(X) are weak functions of X, where Gw(X) incorporates the Pastukhov end-loss expression for the electrons and Cw(X) is essentially the difference between ion and electron sources per unit flux tube, where radial transport is considered a source, and radial electron transport is dependent upon ϕ_e. For the neo-classical transport coefficients presented previously, Cw(X) is a somewhat weak function of X. However, for the full set of coefficients described in Ref. 4, Cw(X) would clearly be strongly dependent upon X in a highly non-linear fashion.

Equation (7.1) is solved in two ways, depending upon the following stability analysis: The problem is to find a solution of x = f(x), using the iterative method $x_{n+1} = f(Xn)$. It is assumed that the exact solution, x, is related to the successive iterations by

$$x_n = x + \varepsilon^n , \tag{7.3}$$

where ε^n is the error at n iterations. Thus:

$$x + \varepsilon^{n+1} = f(x + \varepsilon^n) \cong f(x) + \left.\frac{\partial f}{\partial x}\right|_x \varepsilon^n + O(\varepsilon^{2n}) \tag{7.4}$$

$$x = f(x)$$

$$\varepsilon^{n+1} = \left.\frac{\partial f}{\partial x}\right|_x \varepsilon^n , \tag{7.5}$$

$$\text{which implies} \left| \left.\frac{\partial f}{\partial x}\right|_x \right| \leq 1 \text{ for stability.} \tag{7.6}$$

For the specific case at hand:

$$f(x) = \frac{e^{-x}}{c} \text{ , or} \tag{7.7}$$

$$f(x) = -\ell n(cx) \text{ ,} \tag{7.8}$$

where

$$c = \frac{Cw(x)}{Gw(x)} \text{ .} \tag{7.9}$$

Using (7.7) and (7.6), the stability condition is[11]:

$$e^{-x} \leq c$$
$$x \leq 1 \text{ ,} \tag{7.10}$$

and using (7.8) and (7.5) the stability condition is:

$$c \leq e^{-x}$$
$$x \geq 1 \text{ .} \tag{7.11}$$

The stability boundary is therefore:

$$c_s = e^{-1} \cong 0.3679. \tag{7.12}$$

For $c \geq c_s$, the equation (7.1) is solved using (7.7) and for $c < c_s$, the equation (7.1) is solved using (7.8). Once a set of roots for the potential, ϕ_e, at each mesh point is found using the method, a new Gw(x) and Cw(x) is computed and the procedure is repeated until the fractional change in the x's computed is less than a given error criterion, typically 1×10^{-5}.

As it was previously noted, this method would not be appropriate for strong x behavior of Gw(x) and Cw(x).

REFERENCES

1. J. M. Gilmore, Lawrence Livermore Laboratory, Livermore, CA, UCID-18065 (1979).
2. R. S. Devoto, Computations of MFTF-B Operating Conditions, MFE/TC memo (1979).
3. G. D. Porter, Low β Operation of MFTF-B, MFE/CP/78-313 (1978).
4. R. H. Cohen, Analytic Approximation to Resonant Plateau Transport Coefficients for Tandem Mirrors, Lawrence Livermore Laboratory, Livermore, CA, UCRL-82604, Rev. 1 (1979).
5. D. E. Baldwin, B. G. Logan, and T. K. Fowler, An Improved Tandem Mirror Fusion Reactor, Lawrence Livermore Laboratory, Livermore, CA, UCID-18156 (1979).
6. R. H. Cohen, Time Dependent Tandem Mirror Confinement Studies, Lawrence Livermore Laboratory, Livermore, CA, UCRL-81795, Rev. 1 (1978).
7. S. I. Braginskii, "Transport Processes in a Plasma," Reviews of Plasma Physics I, Consultants Bureau, New York (1965).
8. M. E. Rensink, private communication.
9. R. S. Devoto and J. D. Hanson, SIGV-A Code to Evaluate Plasma Reaction Rates to a Specified Accuracy, Lawrence Livermore Laboratory, Livermore, CA, UCRL-52559 (1978).
10. D. Potter, Computational Physics, John Wiley and Sons, New York (1973).
11. G. E. Gryczkowski, private communication.